MOLECULAR AND CELLULAR BIOLOGY, Aug. 2006, p. 5809–5826 Vol. 26, No. 15
0270-7306/06/$08.00+0 doi:10.1128/MCB.00024-06

Acute Myeloid Leukemia-Associated *Mkl1 (Mrtf-a)* Is a Key Regulator of Mammary Gland Function†

Yi Sun,[1] Kelli Boyd,[2] Wu Xu,[3] Jing Ma,[4] Carl W. Jackson,[5] Amina Fu,[1] Jonathan M. Shillingford,[6]‡ Gertraud W. Robinson,[6] Lothar Hennighausen,[6] Johann K. Hitzler,[7] Zhigui Ma,[1] and Stephan W. Morris[1,5]*

Department of Pathology,[1] Animal Resource Center,[2] Department of Biochemistry,[3] Hartwell Center for Bioinformatics and Biotechnology,[4] and Department of Hematology-Oncology,[5] St. Jude Children's Research Hospital, Memphis, Tennessee 38105; Laboratory of Genetics and Physiology, National Institute of Diabetes and Digestive and Kidney Diseases, NIH, Bethesda, Maryland 20892[6]; and Department of Paediatrics, Division of Haematology/Oncology, Program in Developmental Biology, The Hospital for Sick Children, Toronto, Ontario M5G 1X8, Canada[7]

Received 5 January 2006/Returned for modification 21 February 2006/Accepted 17 May 2006

Transcription of immediate-early genes—as well as multiple genes affecting muscle function, cytoskeletal integrity, apoptosis control, and wound healing/angiogenesis—is regulated by serum response factor (Srf). Extracellular signals regulate Srf in part via a pathway involving megakaryoblastic leukemia 1 (Mkl1, also known as myocardin-related transcription factor A [Mrtf-a]), which coactivates Srf-responsive genes downstream of Rho GTPases. Here we investigate Mkl1 function using gene targeting and show the protein to be essential for the physiologic preparation of the mammary gland during pregnancy and the maintenance of lactation. Lack of Mkl1 causes premature involution and impairs expression of Srf-dependent genes in the mammary myoepithelial cells, which control milk ejection following oxytocin-induced contraction. Despite the importance of Srf in multiple transcriptional pathways and widespread Mkl1 expression, the spectrum of abnormalities associated with Mkl1 absence appears surprisingly restricted.

Megakaryoblastic leukemia 1 (MKL1) was initially identified in acute megakaryoblastic leukemias (AMKLs) that occur in infants and young children due to its involvement in the RBM15-MKL1 fusion protein created by the t(1;22) chromosomal translocation found uniquely in these leukemias (41, 48). As a result of this translocation, the *MKL1* gene (alternatively known as *MAL* [megakaryocytic acute leukemia], *MRTF-A* [myocardin-related transcription factor A], or *BSAC* [basic, SAP {SAF-A/B, acinus, PIAS}, and coiled-coil domain]) (48, 63, 78) from chromosome 22 is juxtaposed and fused in-frame downstream of another novel gene, which encodes RNA-binding motif protein 15 (*RBM15*, alternatively known as *OTT* [one twenty-two]) and is found on chromosome 1; the RBM15-MKL1 fusion protein generated by the 1;22 chromosomal rearrangement is believed to possess oncogenic properties that contribute to the development of AMKL (41, 47).

MKL1 has recently been shown to be a member of a three-protein family that also includes MKL2 (alternatively known as MRTF-B) and myocardin. These myocardin/MKL proteins serve as serum response factor (Srf) coactivators, binding to Srf and strongly activating Srf target genes (13, 50, 65, 76, 78). Serum response factor is a MADS (minichromosome maintenance protein 1, agamous, deficiens, Srf) box transcription factor that regulates serum and growth factor-inducible immediate-early genes, as well as many muscle-specific and -important genes, by binding to serum response elements (SREs), also known as CArG boxes, in their promoter sequences (34, 55, 67). It has been known for more than a decade that ternary complex factor (TCF)—which is comprised of the three ETS-related factors ELK1, SAP1, and SAP2—serves as a coactivator of Srf when it is activated by mitogen-activated protein kinase-mediated phosphorylation. Once stimulated by phosphorylation, TCF activates SRE-containing genes by binding to both the Srf protein and a short DNA sequence element on the 5′ flank of the SRE sequences (75). Inhibition of the TCF-dependent activation of Srf does not, however, result in a complete abrogation of the serum induction of SRE-containing reporter genes, indicating that a second, TCF-independent pathway exists to activate Srf-responsive genes (34). This TCF-independent signaling pathway has been shown to involve Rho GTPases since inhibition of RhoA blocks serum induction of SRE-containing genes and, conversely, constitutively activated RhoA activates SRE-containing gene promoters (30). Until recently, the mechanism by which Srf was regulated in this RhoA-mediated activation pathway remained unclear, given that the Srf protein is constitutively localized to the nucleus and bound to SRE sequences, and no direct modifications of the protein are required for its regulation (34).

The identification of the myocardin/MKL protein family provided a critical break that led to increased understanding of the mechanisms underlying the regulation of TCF-independent Srf activation. The founding member of this family, myocardin, was shown to be expressed specifically in only cardiac and smooth muscle cells and to activate cardiac and smooth muscle gene promoters by associating with Srf, and it was

* Corresponding author. Mailing address: Departments of Pathology and Hematology-Oncology, Thomas Tower, Room 4026, Mail Stop 343, 332 North Lauderdale St., Memphis, TN 38105. Phone: (901) 495-3616. Fax: (901) 495-2032. E-mail: steve.morris@stjude.org.

† Supplemental material for this article may be found at http://mcb.asm.org/.

‡ Present address: Life Sciences and Technology Building, Lab 2203, Molecular, Cellular and Developmental Biology, University of California, Santa Barbara, CA 93106-9610.

suggested to be required for myocardial cell differentiation in *Xenopus* based on studies using an engineered dominant-negative myocardin mutant protein (76); furthermore, myocardin has been shown to regulate the Srf-dependent expression of various smooth muscle genes and to be sufficient to activate smooth muscle genes in nonmuscle cells (17, 21, 38, 39, 80, 82). The three members of the myocardin/MKL family all strongly activate CArG box reporter genes and stably bind Srf (13, 50, 64, 65, 76, 78, 79). In contrast to myocardin, which has cardiac and smooth-muscle-specific expression (17, 21, 76, 82), Mkl1 and Mkl2 are expressed in a wide range of embryonic and adult tissues (41, 63, 78). Dominant-negative Mkl1 blocks Srf reporter gene activation by serum, activated RhoA, and activated mDia, the latter being an effector of Rho GTPase signaling that functions to promote F-actin assembly and Srf activation via the TCF-independent pathway (13, 19, 50, 77). Dominant-negative Mkl1 also blocks serum induction of endogenous Srf target genes, especially those genes without apparent TCF-binding sites (13, 28, 65, 70).

It has recently been found that Rho GTPases regulate Srf via their ability to induce F-actin polymerization, which in turn releases cytoplasmic Mkl1 that is tethered to monomeric G-actin and allows Mkl1 nuclear accumulation, where it fulfills its function as an Srf coactivator (50). As with the mammalian protein, *Drosophila* Mkl1 is responsive to activated Diaphanous (the fly counterpart of mDia), which affects actin cytoskeletal dynamics; consistent with these observations, cell stretching/tension mediated via cytoskeletal changes results in *Drosophila* Mkl1 nuclear accumulation, and cell migration during fly development requires intact Mkl1 and Srf function (69). Mkl2 appears to be a less potent transcriptional coactivator than Mkl1 (78), but complete abrogation of RhoA-induced Srf target gene expression requires inhibition of both Mkl1 and Mkl2 (13), suggesting at least partial redundancy of function between the two proteins. Taken as a whole, these data clearly indicate that the myocardin/MKL protein family mediates signal transduction to Srf in the TCF-independent activation pathway, thereby controlling muscle and immediate-early gene expression; it remains to be determined, however, to what extent the three members of this family serve unique versus redundant transcriptional control functions.

With the exception of a recently published study of *Drosophila* Mkl1 (69), the characterization of Mkl1 function has been performed to date using in vitro cellular systems only; thus, the functions of the protein in vivo are not yet fully clear. Here we investigate the physiological roles of mammalian Mkl1 during development and in adults using gene-targeting techniques to generate Mkl1 null mice. We demonstrate an absolute requirement for Mkl1 function in the normal mammary gland physiologic responses that prepare the gland for lactation in the latter stages of pregnancy and maintain lactation during the postpartum period. The absence of Mkl1 is associated with the development of an involution-like phenotype in the mammary tissue that precludes the ability of Mkl1$^{-/-}$ mothers to sustain the nutritional requirements of their progeny; in addition, Mkl1 deletion significantly impairs the expression of Srf-dependent muscle genes in the mammary myoepithelial cells, which normally contract and cause milk ejection in response to suckling and resultant oxytocin release. We also demonstrate that, although Mkl1 is not absolutely required for embryonic heart development, a subset of our Mkl1$^{-/-}$ embryos suffer death at approximately embryonic day 10.5 (E10.5) due to myocardial cell necrosis that may reflect an impaired ability of the myocardium to respond to environmental stresses. In contradistinction to the global effects upon transcriptional control exerted by Srf, the relatively restricted phenotypic abnormalities we report here help to define the unique and essential roles that Mkl1 plays in modulating Srf function and regulating mammalian development and function.

MATERIALS AND METHODS

Generation and analysis of *Mkl1*$^{-/-}$ mice. A genomic DNA fragment encompassing the 3′ portion of the mouse *Mkl1* gene from strain 129SvEv mice (Stratagene) was isolated. An *Mkl1* targeting vector was constructed using this DNA fragment to delete coding exons 9 to 14, inclusive, which encode amino acids 240 to 794 of the Mkl1 protein. The *Mkl1* targeting vector (10 μg) was electroporated into embryonic stem (ES) cells from strain 129Sv mice (Specialty Media), which were selected in G418 (Invitrogen) and ganciclovir (Roche Biosciences). Two hundred ES clones were screened by Southern blot analysis for homologous recombination events within the *Mkl1* locus. Genomic DNAs from these clones were digested with BstEII, then Southern hybridization using a 500-bp intronic probe located external to the 5′ extent of the targeting construct was carried out. Four ES cell clones were shown to be both correctly targeted and karyotypically normal. These four clones were injected into C57BL/6 blastocysts, and germ line transmission of the deleted *Mkl1* allele was obtained from chimeric males derived from two individual ES cell clones. The genotypes of the mice were determined by PCR using primer 1 (5′ TGCTTGCATGTATGGCTGTT 3′) and primer 2 (5′ TGTTTGGTGCTCAGCAGTTC 3′) from the intronic sequences between exons 14 and 15 and primer 3 (5′ CAGAAAGCGAAGGAGCAAAG 3′) from the *neo* resistance gene; the PCR generated 340-bp wild-type and 500-bp targeted bands.

Hemizygous or homozygous Mkl1-deficient mice were mated at approximately 6 weeks of age. For timed-mating pregnancies, *Mkl1*$^{-/-}$ male and female mice were mated overnight and the females with copulation plugs were removed from the breeding cages the next morning and either sacrificed to collect embryos at various times during pregnancy or observed until delivery. For oxytocin and prolactin injections, oxytocin (600 milliunits/kg of body weight/day) (Sigma) or prolactin (0.5 mg/mouse/day) (NIDDK National Hormone & Peptide Program [www.humc.edu/hormones]) were injected intraperitoneally every 8 h for 10 days beginning on postpartum day 3.

Immunoprecipitations and immunoblotting. For immunoprecipitations, mouse embryonic fibroblasts (MEFs) were lysed in radioimmunoprecipitation assay buffer, and the protein in the lysates was immunoprecipitated with an anti-Mkl1 polyclonal rabbit antiserum kindly provided by Ron Prywes (13). The precipitated proteins were immunoblotted with the same anti-Mkl1 serum, using a 1:1,500 dilution.

Histological analysis. For light microscopic histological examination, mammary gland tissues were fixed in 4% neutral buffered formalin, embedded in paraffin, and sectioned at 4-μm intervals. After a graded alcohol dehydration and two xylene-clearing stages, the sections were stained with conventional hematoxylin-eosin reagents. For electron microscopy, the mammary glands were processed, embedded, sectioned, and examined using previously described methods (24, 51).

Immunohistochemistry. Slides of 4-μm-thick sections cut from formalin-fixed paraffin-embedded tissues were deparaffinized in xylene, and immunohistochemistry was performed with a DAKO autostainer following the manufacturer's instructions. For α-smooth muscle actin (SMA) staining, monoclonal mouse anti-human α-smooth muscle actin (clone 1A4; catalog no. M0851), which also reacts with the mouse protein, was obtained from DAKO and complexed to biotin prior to use with an animal research kit (catalog no. K3954; DAKO). Mouse immunoglobulin (Ig) G2a kappa (clone C1.18.4; catalog no. 557274; Pharmingen) was used as a negative control at the same concentration as the SMA antibody. Heat-induced epitope retrieval was performed at >95°C for 30 min in citrate buffer (pH 6.0) (catalog no. 00-5000; Zymed). Slides were allowed to cool for 30 min and were placed in Tris-buffered saline (catalog no. S3006; DAKO) for 10 min prior to the assay. Endogenous peroxidase activity was blocked by incubation with 3% H_2O_2 (Humco) for 5 to 10 min. The slides were then incubated with biotinylated anti-SMA antibody (1:20, 30 min) or with the biotinylated negative control antibody. Slides were subsequently incubated for 10 min with streptavidin conjugated to horseradish peroxidase (catalog no. K1016;

DAKO) and for 10 min with substrate containing the chromogen 3,3′ diaminobenzidine tetrahydrochloride (catalog no. K3468; DAKO). The slides were counterstained for 3 min with a 1:5 dilution of hematoxylin (catalog no. S3309; DAKO), dehydrated, and placed on coverslips.

Assessment of apoptosis. Terminal deoxynucleotidyltransferase-mediated dUTP-biotin nick end labeling (TUNEL) assays were performed using the Dead End kit (catalog no. PRG7130; Promega) adapted for use on the Discovery stainer (Ventana Medical Systems, Tucson, Ariz.). Slides of 4- to 6-μm-thick sections cut from formalin-fixed, paraffin-embedded tissues were baked at 60°C for 30 min and placed on the Discovery stainer. All steps of the Dead End kit protocol were followed exactly, except that deparaffinization of the slides was programmed as part of the TUNEL protocol on the stainer, and an additional step consisting of a 10-min incubation with proteinase K (catalog no. S3020; DAKO) at room temperature was included prior to terminal transferase incubation.

Microarray analysis. Total RNA was extracted with RNA STAT-60 (Tel-Test, Inc.) according to the manufacturer's instructions. For differential expression analysis, the mammary tissues from *Mkl1*$^{-/-}$ ($n = 3$) and wild-type ($n = 3$) mice were obtained at postpartum day 5. RNA quality and integrity prior to microarray analysis were assessed using the Agilent 2100 Bioanalyzer. Double-stranded cDNA was synthesized from total RNA using the SuperScript double-stranded cDNA synthesis kit (Life Technologies) and primer T7-dT24-DNA (5′ GGCC AGTGAATTGTAATACGACTCACTATAGGGAGGCGG 3′) per the manufacturer's instructions. Using this double-stranded cDNA as a template, a labeled antisense cRNA was synthesized with biotinylated UTP and CTP by in vitro transcription using a T7 RNA transcript labeling kit (ENZO Diagnostics). The labeled cRNA was passed through a CHROMASPIN-100 column (Clontech), fragmented by heating and ion-mediated hydrolysis, and then used for hybridization to the Mouse Genome 430 2.0 GeneChip oligonucleotide microarrays (Affymetrix), which contain 45,037 probe sets (~34,000 genes). After hybridization, the oligonucleotide arrays were washed and stained with phycoerythrin-conjugated streptavidin (Molecular Probes). The arrays were then scanned with a laser confocal scanner (Agilent), gene expression signals were scaled to a target intensity of 500, and detection values were determined with the default settings of Affymetrix Microarray Suite 5.0.

Statistical analysis. Unless otherwise specified, R 2.0.1 software (R Foundation for Statistical Computing, Vienna, Austria) was used for both identification and functional classification of differentially expressed genes. First, probe sets designated by Affymetrix Microarray Suite 5.0 as "absent" in all six arrays were filtered out (this eliminated 25,888 probe sets, leaving 19,149 probe sets for further analysis). Then, the local-pooled-error method (33) and q-value estimation for the false discovery rate (72) available in the local-pooled-error and *q* value packages, respectively, from the Bioconductor project (27), were used to identify genes that were differentially expressed between *Mkl1*$^{-/-}$ and wild-type mice.

Two hundred forty-eight probe sets, representing 182 different genes, were identified as being significantly differentially expressed at *q* values of <0.05. These 248 probe sets were then functionally classified using the biological process categories of the Gene Ontology Consortium (3). Fisher's exact test was used to determine the overrepresented gene ontology biological process categories in these probe sets, and the *P* values were corrected for multiple testing using the false discovery rate controlling procedure of Benjamini and Hochberg (11).

Real-time PCR quantification of gene expression. cDNAs were generated from 200 ng of total RNA prepared from either whole mammary glands or purified mammary myoepithelial cells using SuperScript II RNase H− reverse transcriptase (Invitrogen) and nonamer random primers. Beta-actin was used as an internal standard. Real-time PCR was performed with an ABI Prism 7700 sequence detector system (Applied Biosystems). Oligonucleotide primers and a TaqMan probe were designed for each gene using Primer Express version 2.0 software (Applied Biosystems). Primer sequences are available from the authors upon request. The expression of each gene examined by real-time PCR was normalized relative to the expression of beta-actin.

Promoter sequence analysis. One kilobase of the promoter sequences was sought from each of the 48 down-regulated genes (65 probe sets) that were identified using the University of California Santa Cruz (UCSC) genome browser (UCSC mouse database release mm5, May 2004); the upstream sequences were available for 37 of these genes (42 probe sets). We then used Clover (*cis*-element overrepresentation) (23) to scan a precompiled library of 542 vertebrate motifs from the TRANSFAC Professional database (46), version 8.3, against the 1-kb promoter sequences of each of the 37 genes to identify significantly overrepresented motifs. A *P* value threshold of less than 0.01 was used to determine significance.

Purification of mammary myoepithelial cells. Myoepithelial cells of mammary glands were isolated from mice on postpartum day 5 as described previously in the literature (54), with modifications. Briefly, mammary gland tissues dissected from mice that had been decapitated were minced and washed in Ca^{2+}- and Mg^{2+}-free phosphate-buffered saline (PBS). The minced tissues were incubated with 2,000 protease units/ml of Dispase (Invitrogen) in Dulbecco's modified Eagle's/F-12 medium (Sigma) containing 100 IU/ml penicillin (Sigma) and 100 μg/ml streptomycin (Sigma), supplemented with 5% fetal bovine serum (ICN) and 0.0001% DNase I (Sigma) for 90 min on a shaker at 37°C. The tissues were washed with PBS, then incubated for 30 min at 37°C in PBS. Thereafter, the tissues were again washed with PBS prior to digestion with 0.5 to ~1.0 mg/ml collagenase (Type III; Worthington) in the medium described above for 15 min at 37°C. The digested tissue was washed with PBS, and cells were dissociated in PBS containing 0.02% EDTA using a Pasteur pipette. The cell suspension in PBS was serially filtered with nylon mesh (pore sizes, 150 and 25 μm), and the solution of filtrate was replaced with Dulbecco's modified Eagle's/F-12 medium. The cell suspension was layered on top of a Percoll discontinuous gradient (1.050, 1.060, 1.065, 1.070, 1.075, 1.080 g/ml) in normal Ringer's solution containing 2% Ficoll, 20 mM HEPES (pH 7.5) and 2% bovine serum albumin (Sigma) and centrifuged for 30 min at 800 × *g*. Myoepithelial cells, which sediment at a density of 1.070 to 1.080 g/ml, were separated from secretory epithelial cells (sedimentation at <1.065 g/ml), collected, washed three times with cold PBS (containing 1% FCS), and then filtered through 56-μm-pore-size gauze (Henry Simon, Ltd., Stockport, United Kingdom) and counted. The cells were labeled with anti-CD10 primary rabbit IgG antibody (Santa Cruz Biotechnology) at a ratio of 1×10^6 cells/10 μl antibody in a 0.5-ml final volume for 10 min at 4°C, with occasional gentle inversion. The cells were then washed twice by carefully adding 10 ml PBS buffer (PBS, pH 7.2, with 0.5% bovine serum albumin and 2 mM EDTA) and centrifuged at 300 × *g*, and then the supernatant was completely removed. The cell pellet was resuspended in 80 μl of PBS buffer per 10^7 cells, and MACS goat anti-rabbit IgG MicroBeads (20 μl; Miltenyi Biotec) were added and incubated for 15 min at 6 to 12°C. Thereafter, the cells were washed with 20 ml PBS buffer and resuspended in 500 μl buffer per 10^8 cells, then purified by magnetic separation per the manufacturer's instructions.

RESULTS

Generation of Mkl1-knockout mice. The *Mkl1* gene was disrupted by homologous recombination in murine ES cells, with replacement of exons 9 to 14, inclusive, by a neomycin resistance cassette (Fig. 1A). These deleted exons encode the amino acids (240 to 794) that comprise the entirety of the basic, glutamine-rich, SAP, and coiled-coil motifs of Mkl1, as well as a portion of the transactivation domain of the protein. Germ line transmission of the deleted *Mkl1* allele was achieved from chimeric males derived from two individually targeted unique ES cell clones; the phenotypic abnormalities reported herein were identical in each of the two lines of *Mkl1* knockout mice generated using these targeted ES cells. *Mkl1* hemizygous (+/−) mice appeared healthy throughout their lives and were intercrossed to obtain homozygous Mkl1-deficient (−/−) animals, as confirmed by Southern blot analysis of tail DNA samples (Fig. 1B). The null mutation of *Mkl1* in *Mkl1*$^{-/-}$ mice was confirmed by Western blotting analysis of lysates from MEFs isolated from E13.5 embryos, which revealed the complete absence of detectable Mkl1 protein expression (Fig. 1C). *Mkl1* hemizygous and homozygous null viably born pups and adult mice were indistinguishable from their wild-type littermates at birth; their appearance was grossly normal, and their organs were found to be histologically normal by light microscopy.

Mkl1 deficiency results in partial embryonic lethality caused by cardiac cell death. In vitro studies have suggested that Mkl1 is a transcriptional cofactor that strongly activates Srf-responsive muscle-specific and -important gene promoters by physically associating with Srf (13, 50, 78). In addition, the

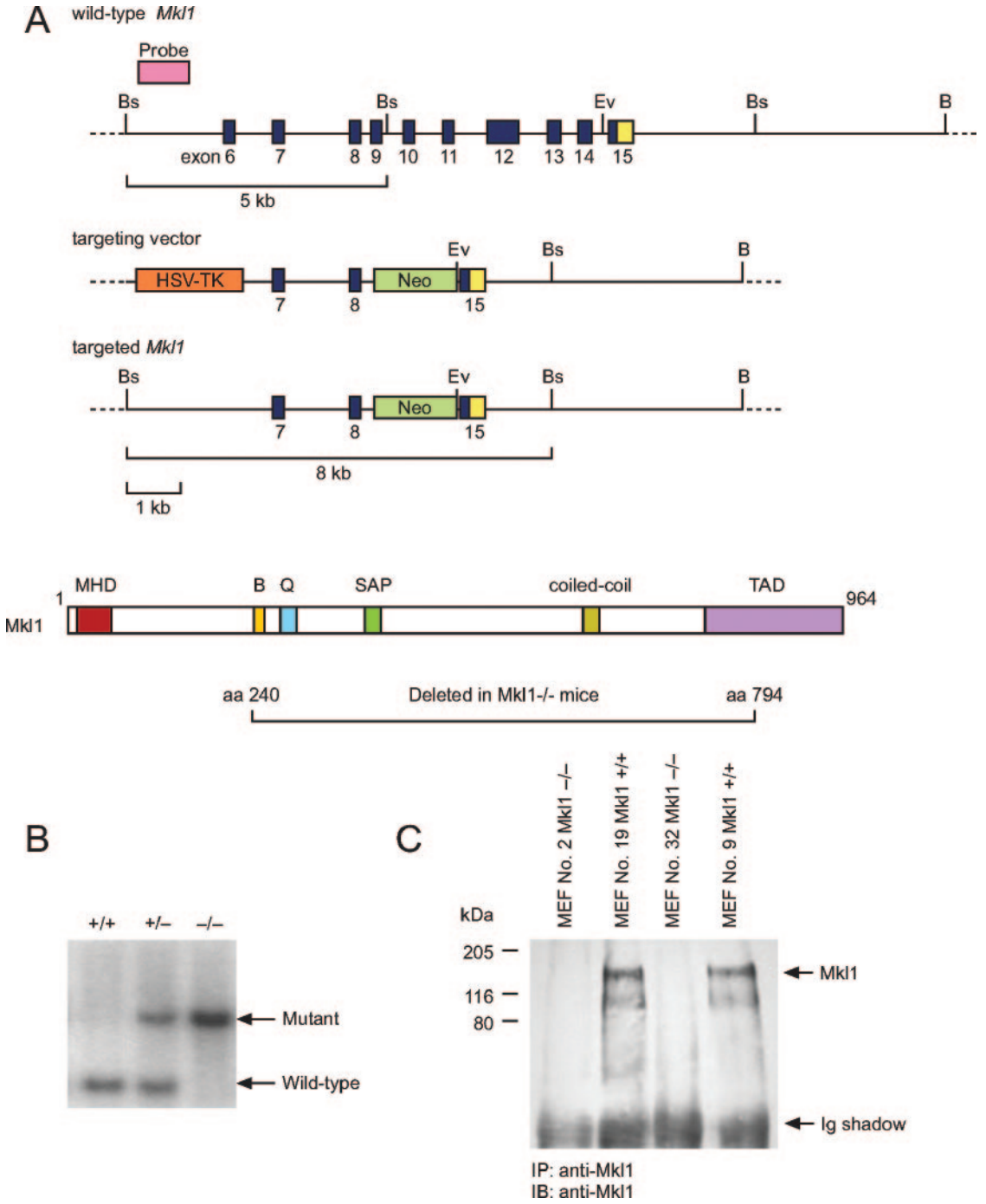

FIG. 1. Generation of *Mkl1*$^{-/-}$ mice. (A) Targeted disruption of *Mkl1*. The genomic sequences containing *Mkl1* exons 9 to 14, inclusive, were replaced with a neomycin resistance cassette. The 5′ probe used for Southern blot analysis and the expected BstEII DNA restriction fragments are indicated. Bs, BstEII; EV, EcoRV; B, BamHI. The schematic of Mkl1 shows the portion of the protein encoded by the deleted exons. MHD, myocardin/MKL homology domain; B, basic amino acid-rich region; Q, glutamine-rich region; SAP, putative DNA-binding/chromatin association domain; CC, coiled-coil domain; TAD, transcriptional activation domain; aa, amino acid. (B) Southern blot analysis of mouse tail genomic DNA. The expected DNA fragments for the targeted and wild-type alleles are 8 and 5 kb, respectively. +/+, wild type; +/−, heterozygote; −/−, homozygote. (C) Sequential immunoprecipitation (IP)/immunoblot (IB) analysis using an Mkl1-specific rabbit polyclonal antibody. Note the absence of Mkl1 protein from homozygously targeted (−/−) MEFs compared to wild-type (+/+) MEFs, both of which were isolated from E13.5 embryos.

overexpression of Mkl1 has been associated with cell survival; specifically, this prosurvival effect is able to partially rescue the cell death of Traf-2 and -5 double-deficient MEFs induced by tumor necrosis factor (63).

These findings suggest that Mkl1 could play a role in the development and/or survival of cardiac, smooth, and skeletal muscle tissues; however, no readily apparent abnormalities in muscle development or function were discernible in *Mkl1*$^{-/-}$

A

Genotype of progeny of Mkl1 heterozygote (+/–) intercrosses

Genotype	Number of progeny	Percentage (expected percentage)
+/+	66	28.8 (25)
+/–	129	56.4 (50)
–/–	34	14.8 (25)
Total	229	100

B

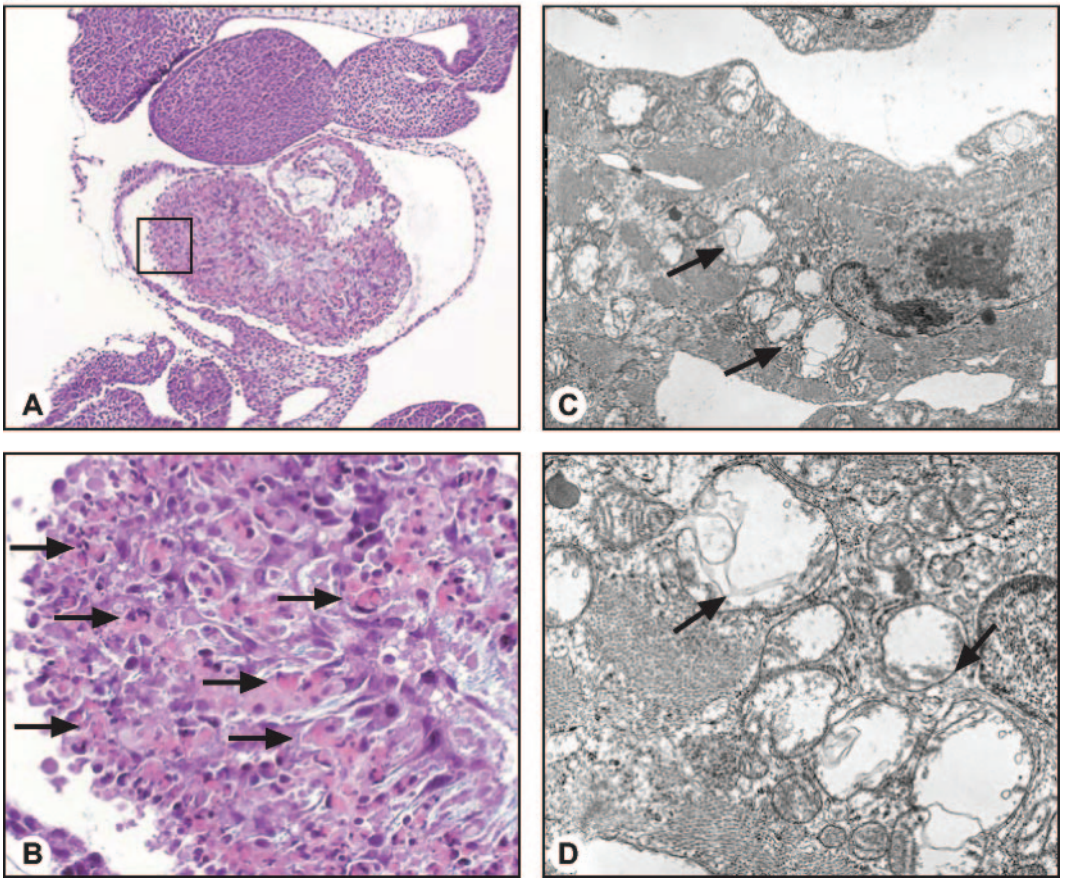

FIG. 2. Partial embryonic lethality associated with abnormal cardiogenesis due to Mkl1 absence. (A) Mendelian frequency of the progeny born to Mkl1 hemizygote intercrosses. Note that only 14.8% of the offspring are homozygous *Mkl1*$^{-/-}$ mice (34 of a total of 229 pups), which is less than the expected frequency (25%), indicating partial embryonic lethality in embryos that lack Mkl1. (B) Cardiac sections of E10.5 *Mkl1*$^{-/-}$ mouse embryos. (A and B) Hematoxylin and eosin staining. (A) Magnification, 40×. (B) Magnification (400×) of boxed area in panel A. There is substantial necrosis of myocardial cells of the ventricular and atrial walls, which appear as hyalinized eosinophilic cells with shrunken and fragmented nuclei (arrows). (C and D) Electron microscopy of E10.5 *Mkl1*$^{-/-}$ embryonic heart. Mitochondria (arrows) of the affected myocardiocytes are markedly swollen and are shown in various stages of degeneration. There is no cytosolic swelling or change in nuclear morphology suggestive of an apoptotic cell death process; similarly, no electron microscopic evidence of autophagic death (i.e., double-membraned autophagosomes or autophagolysosomes in the cytoplasm) was observed.

pups or adult mice. Based on the hypothesis that defects in the ability of mesenchymal tissues to develop normally to specific muscle lineages might result in a partial fetal wastage of *Mkl1*$^{-/-}$ embryos, we examined the integrity of embryonic development in the absence of Mkl1. To analyze the Mendelian frequency of viable *Mkl1*$^{-/-}$ births, we genotyped the progeny from *Mkl1*$^{+/-}$ hemizygote intercrosses. This analysis revealed that only 34 (14.8%, rather than the expected 25%) *Mkl1*$^{-/-}$ pups were born out of a total of 229 progeny from these crosses (Fig. 2A), indicating that approximately 40%

(40.8%, if Mendelian genetics were to hold exactly true) of *Mkl1*$^{-/-}$ fetuses died during embryogenesis.

Isolation of embryos ranging from developmental stages E10 to E18.5 from intercrosses between *Mkl1*$^{-/-}$ male and female mice revealed that 35% of E10.5 *Mkl1*$^{-/-}$ embryos suffered dilated cardiac atrial and ventricular chambers, as well as dilation of their outflow vessels (aortic and pulmonary arteries) (data not shown). In addition, edema was seen around the hearts within the pericardial space, consistent with effusions that may have resulted from abnormalities of the cardiac musculature that were also observed (see below) and/or heart failure (Fig. 2B, panel A). By contrast, the remaining 65% of *Mkl1*$^{-/-}$ mice, as well as *Mkl*$^{+/-}$ and wild-type, embryos showed no evidence of cardiac abnormalities (data not shown). Similarly, no evident differences were observed histologically between postnatal wild-type, *Mkl1*$^{+/-}$, and *Mkl1*$^{-/-}$ mice in the overall development of the cardiac structures; for example, the thicknesses of both the atrial and ventricular myocardial layers were not substantively altered in the absence of Mkl1. Thus, Mkl1 function is not required for the specification and formation of the heart from mesenchymal precursor tissues.

By contrast, however, Mkl1 function was apparently required to maintain the integrity of the myocardium in the subset of *Mkl1*$^{-/-}$ embryos that succumbed during development; specifically, histological analyses demonstrated myocardial cell death associated with coagulative necrosis in the atrial and ventricular walls (Fig. 2B, panels A and B). Examination of E10.5 and earlier embryos by in situ TUNEL assay revealed indistinguishable numbers of apoptotic cardiac cells in *Mkl1*$^{-/-}$ and wild-type embryos (data not shown), suggesting that apoptosis was not a major cause of the myocardial cell death. Electron microscopic examination of the cardiac musculature also failed to show the typical signs of apoptotic cell death (nuclear condensation, association of chromatin with the nuclear periphery, DNA fragmentation, membrane blebbing, lack of major ultrastructural changes of the cytoplasmic organelles, engulfment and lysosomal degradation of dying cells by phagocytes) (Fig. 2B, panels C and D). Likewise, no morphological evidence indicative of autophagic cell death (the presence in the cytoplasm of dying cells of double-membrane structures known as autophagosomes, as well as autophagolysosomes resulting from the fusion of autophagosomes with lysosomes) was observed in electron microscopic images of the myocardium. Although neither global cytosolic swelling nor substantial changes in nuclear morphology were identified, the mitochondria of the myocardiocytes were markedly swollen and in various states of degeneration (Fig. 2B, panels C and D). These results suggest a nonprogrammed (i.e., neither apoptotic nor autophagic) mechanism of myocardial cell death in *Mkl1*$^{-/-}$ embryos that most closely resembles cellular necrosis (7, 35). No other apparent abnormalities were observed in these *Mkl1*$^{-/-}$ embryos up to the time of their death, or in the *Mkl1*$^{-/-}$ embryos that survived to term.

Failure-to-thrive syndrome and death of pups born to *Mkl1*$^{-/-}$ mothers. As noted, approximately 60% of *Mkl1*$^{-/-}$ mice were viable following full-term pregnancies. These animals were born with an equal male-to-female ratio. Extensive gross and histological examination revealed no evident abnormalities, and *Mkl1*$^{-/-}$ mice that attained adulthood appeared indistinguishable from their wild-type or hemizygote adult littermates.

Similarly, the fecundity of *Mkl1*$^{-/-}$ mice was found to be normal compared with wild-type and hemizygous mice; no significant differences were observed in the numbers of litters or pups per litter born to intercrosses between *Mkl1*$^{-/-}$ males or females with wild-type, hemizygous, or *Mkl1*$^{-/-}$ breeding partners. Thus, *Mkl1*$^{-/-}$ males were fertile, and *Mkl1*$^{-/-}$ females possessed no inherent gestational or parturition defects. However, pups born to *Mkl1*$^{-/-}$ mothers failed to thrive. Although initially comparable in size and appearance to pups born to wild-type or *Mkl1*$^{+/-}$ mothers, pups born to *Mkl1*$^{-/-}$ mothers failed to gain weight following their first week of life (Fig. 3A). Pregnant *Mkl1*$^{-/-}$ mice were observed to build typical nests and, after delivery, the offspring were cleaned and present in the nest. In addition, the mothers quickly retrieved offspring that were moved outside of the nest. Thus, the maternal behavior of *Mkl1*$^{-/-}$ females appeared normal.

Despite the ostensibly normal maternal behavior, the offspring of *Mkl1*$^{-/-}$ females died 14 to 17 days postpartum. The death of the pups occurred independently of their genotype but tracked with the genotype of their mothers. Therefore, we performed experiments in which we placed 8-day-old wild-type pups with *Mkl1*$^{-/-}$ nursing females and 8-day-old *Mkl1*$^{-/-}$ pups with wild-type nursing females to determine the consequences of such a switch (Fig. 3). Consistent with an abnormality associated specifically with the *Mkl1*$^{-/-}$ dams, all *Mkl1*$^{-/-}$ pups removed from their *Mkl1*$^{-/-}$ birth mothers and placed with wild-type dams survived to weaning and adulthood, whereas no wild-type pups placed with *Mkl1*$^{-/-}$ mothers survived to weaning (Fig. 3D). Taken as a whole, these results suggest the inability of *Mkl1*$^{-/-}$ mothers to support the nutritional requirements of their suckling pups to the point at which they can be weaned.

Treatment of *Mkl1*$^{-/-}$ nursing females with oxytocin and/or prolactin fails to correct the failure-to-thrive syndrome. To help rule out the possibility that hormones critical for normal lactation and nursing are deficient in *Mkl1*$^{-/-}$ females, we injected five *Mkl1*$^{-/-}$ females intraperitoneally with oxytocin (600 milliunits/kg/day) and/or prolactin (0.5 mg/mouse/day) every 8 h from postpartum day 3 to postpartum day 13. Analysis of the growth curves of suckling pups born to these *Mkl1*$^{-/-}$ mothers demonstrated that the injections of neither oxytocin alone, prolactin alone, nor the two together, had any effect on the growth or survival of the offspring, with all pups dying within 17 days of birth (data not shown).

Additional evidence suggesting that the hormonal milieu of *Mkl1*$^{-/-}$ females is probably normal was provided by examination of the pituitary glands of these animals, which demonstrated an increase in the size of the pars intermedia at postpartum day 9 compared to wild-type postpartum controls; by contrast, examination of the pituitary glands of virgin and 19-day-pregnant females showed no differences in the size of the pars intermedia between *Mkl1*$^{-/-}$ and wild-type females (see the figure in the supplemental material). In the mouse, melanocyte-stimulating hormone, which is synthesized by the pars intermedia, is normally released after suckling stimuli, in turn prompting the release of prolactin from the pars distalis of the pituitary to help maintain lactation (73). Although we cannot unequivocally rule out more subtle defects in reproduc-

A

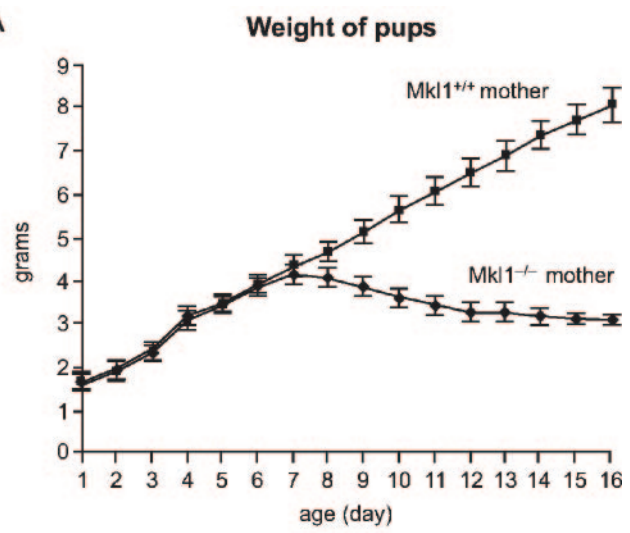

B

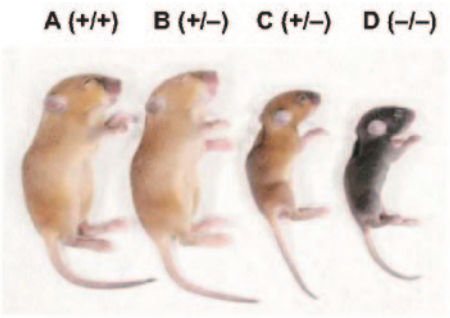

C

Mating (female x male)	Age	Number of progeny	Survival rate (%)
+/– x +/–	7 wks	90	97
+/– x –/–	7 wks	95	96
–/– x +/–	7 wks	96	0
–/– x –/–	7 wks	102	0

D

Nursing mothers	8-day-old pups	Survival rate (%)
4 Mkl1 –/–	24 wild-type	0
4 Wild-type	24 Mkl1–/–	100

FIG. 3. Failure-to-thrive syndrome of pups suckling *Mkl1*$^{-/-}$ mothers. (A) Weight gain of pups born to intercrosses between either *Mkl1*$^{-/-}$ males × *Mkl1*$^{+/+}$ females or *Mkl1*$^{+/+}$ males × *Mkl1*$^{-/-}$ females at each time point indicated during the postnatal period. Each data point represents the average weight (in grams) of 20 pups. Note that pups of *Mkl1*$^{-/-}$ mothers failed to gain weight after their first week of life. (B) Photographs of 11-day-old pups. Pup A (*Mkl1*$^{+/+}$) was born from a hemizygote (+/−) parental intercross, pup B (Mkl1 +/−) was born from a hemizygote female (+/−) × null male (−/−) cross, pup C (Mkl1 +/−) was born from a null female (−/−) × hemizygote male (+/−) cross, and pup D (*Mkl1*$^{-/-}$) was born from a null male (−/−) × null female (−/−) intercross. All four mice were kept with their respective birth mothers during the entire 11-day postnatal period. *Mkl1*$^{-/-}$ pups born in the same litters as pups A and B, but not C, gained weight and appeared healthy, similar to their wild-type and *Mkl1*$^{+/-}$ littermates (not shown); all littermates of pup D exhibited a failure-to-thrive phenotype. (C) Survival rates of the progeny from intercrosses of parents with various Mkl1 genotypes. Male/female (7-week-old) breeding pairs with the indicated genotypes produced the number of progeny shown. The pups born to these crosses were kept with their birth mothers and observed for a 16-day postnatal period. Note that Mkl1 absence does not alter the fecundity of either male or female parents and, importantly, that no progeny of *Mkl1*$^{-/-}$ mothers survived the postnatal observation period. (D) Survival rates of 8-day-old pups (wild-type or *Mkl1*$^{-/-}$) after placing them with *Mkl1*$^{-/-}$ or wild-type nursing foster mothers. The pups were interchanged between their birth mothers at postpartum day 8, then observed for an additional 8-day period. Note that the ability to survive the immediate postnatal period is independent of the Mkl1 status of the pups but correlates with the genotype of the foster mothers.

tive and/or postnatal endocrinology, the inability of exogenously administered oxytocin and prolactin to reverse the weight loss and death of pups that suckle *Mkl1*$^{-/-}$ mothers, together with the apparent physiologic, compensatory enlargement of the pars intermedia observed in *Mkl1*$^{-/-}$ females during the postpartum period, support instead the presence of primary, intrinsic mammary gland defects that prevent normal responses to the hormones that control lactation and nursing in females lacking Mkl1.

Identification of genes differentially expressed in the mammary glands of *Mkl1*$^{-/-}$ mice during lactation. As an initial step to explore mammary gland function in *Mkl1*$^{-/-}$ females, we performed gene expression profiling by microarray analysis. Total RNA from mammary glands in early lactation (postpartum day 5) was extracted and analyzed using mouse genome oligonucleotide microarrays (430v2.0; Affymetrix). The RNA samples were taken in triplicate from mammary glands from three individual *Mkl1*$^{-/-}$ mice as well as three control wild-type mice at postpartum day 5. Data analysis showed that 248 probe sets, representing 182 different genes, were differentially expressed between *Mkl1*$^{-/-}$ and wild-type mammary gland tissues (Fig. 4; see Tables S1 and S2 in the supplemental material). In order to establish correlations between gene function and gene expression patterns, the transcripts with known function were assigned to categories, and statistically significant (adjusted P value, <0.05) associations among specific gene functions were identified using gene ontology biological process categories. This analysis revealed that the 182 differentially expressed gene transcripts cover 14 biological processes (see Table S2 in the supplemental material) that were significantly altered in *Mkl1*$^{-/-}$ mammary glands. These processes include cell motility, muscle contraction and development, cell death regulation, responses to stress and biotic stimuli (including acute-phase responses), control of cellular homeostasis (especially concerning inorganic di- and trivalent metal cation [e.g., iron and zinc] transport), regulation of cell proliferation, acetyl-coenzyme A (CoA) and acetate metabolism, cell surface receptor-linked signal transduction, nucleic acid metabolism, nitric oxide-mediated signal transduction, and the regulation of peptidyl-tyrosine phosphorylation by Egf and Pdgf (see Table S2 in the supplemental material). The three most significant differentially represented functional processes seen in *Mkl1*$^{-/-}$ and wild-type mammary tissues involved in muscle contraction, the acute-phase response, and

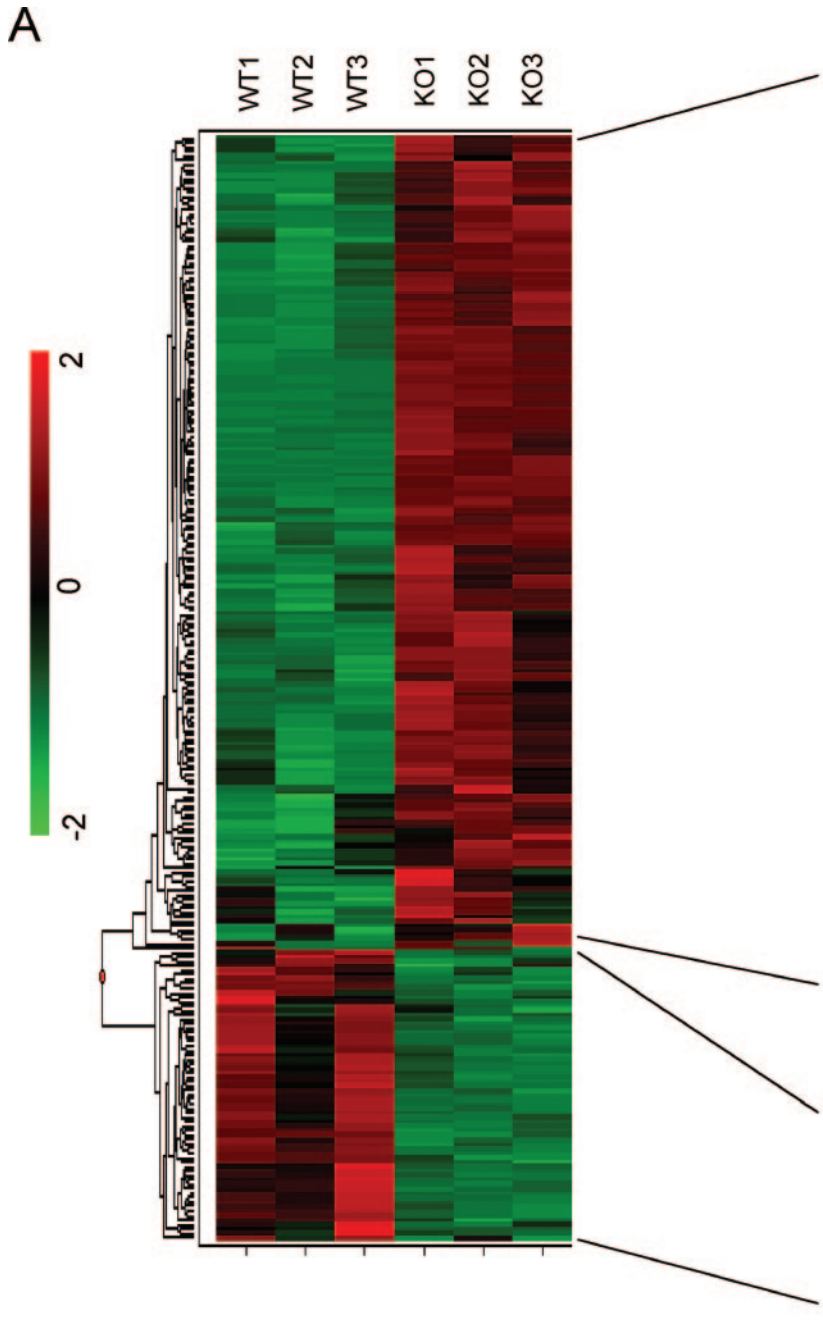

Up-regulated mammary gland involution genes

Probe Set ID	Gene Symbol	Fold, KO vs. WT
1417290_at	Lrg1	82.0
1449326_x_at	Saa2	38.6
1428572_at	Basp1	38.1
1416523_at	Rnase1	27.6
1452114_s_at	Igfbp5	21.7
1417130_s_at	Angptl4	14.7
1420438_at	Orm2	13.9
1417852_x_at	Clca1	12.0
1417268_at	Cd14	10.4
1418283_at	Cldn4	10.4
1450826_a_at	Saa3	7.7
1416576_at	Socs3	7.4
1455899_x_at	Socs3	6.9
1448377_at	Slpi	5.9
1418021_at	C4	5.4
1451737_at	Pik3r1	5.3
1417850_at	Rb1	4.5
1425249_a_at	Tyro3	4.3
1425476_at	Col4a5	4.2
1425475_at	Col4a5	3.5
1417494_a_at	Cp	3.4
1423233_at	Cebpd	3.4
1421752_a_at	Serpinb5	3.3
1418981_at	Casp12	3.1
1448734_at	Cp	3.0
1455393_at	Cp	3.0
1417495_x_at	Cp	2.9
1450355_a_at	Capg	2.8
1418374_at	Fxyd3	2.7
1448272_at	Btg2	2.6
1422438_at	Ephx1	2.6
1460243_at	Sptlc2	2.5
1417455_at	Tgfb3	2.5
1417496_at	Cp	2.4
1423456_at	Bzw2	2.2
1418364_a_at	Ftl1	2.2
1460700_at	Stat3	2.2
1450009_at	Ltf	2.2
1460235_at	Scarb2	2.1
1426587_a_at	Stat3	2.1
1454758_a_at	Tgfb1i4	2.1
1451310_a_at	Ctsl	2.1

Down-regulated muscle contraction genes

Probe Set ID	Gene Symbol	Fold, KO vs. WT
1417917_at	Cnn1	-5.4
1448962_at	Myh11	-3.3
1427735_a_at	Acta1	-2.6
1452670_at	Myl9	-2.4
1416889_at	Tnni2	-2.3
1425028_a_at	Tpm2	-2.3
1427520_a_at	Myh1	-2.1

FIG. 4. Differential gene expression in *Mkl1*$^{-/-}$ mammary glands compared with wild-type mammary tissue. (A) Hierarchical clustering of the 248 probe sets (representing 182 different genes) that are significantly differentially expressed (q value, <0.05) between mammary tissue from *Mkl1*$^{-/-}$ and *Mkl1*$^{+/+}$ mice. Mammary glands from either *Mkl1*$^{-/-}$ or *Mkl1*$^{+/+}$ dams (three of each) at postpartum day 5 were collected and used for expression profiling analyses. Each column shown in the figure represents one mammary gland tissue sample, and each row represents a probe set. Expression levels are normalized for each probe set, where the mean is zero; expression levels greater than the mean are shown in red, and levels less than the mean are in green. Increasing distance from the mean is represented by increasing color intensity. Two subgroups of the entire 248-probe set involving genes known to be up-regulated during normal mammary gland involution or involved in normal muscle function are shown to the right of the heat map. The DecisionSite for Functional Genomics (version 8.1) module (Spotfire, Inc., Somerville, MA) was used for the hierarchical clustering. Detailed information concerning all 248 probe sets is shown in Table S1 in the supplemental material. KO, knockout; WT, wild type. (B) Known mammary gland involution genes overexpressed in *Mkl1*$^{-/-}$ mammary glands from nursing mothers at postpartum day 5.

transition metal ion homeostasis (P value, 0.000067 for each of the three). For example, of a total of 53 genes present on the microarray chips known to be important for muscle contraction, the expression of 7 was reduced in *Mkl1*$^{-/-}$ mammary glands (Fig. 4A). Among 506 stress-regulated transcripts, 16 genes were altered in *Mkl1*$^{-/-}$ mammary glands, and 6 of these 16 transcripts represent acute-phase response-associated genes (see Table S2 in the supplemental material). Of 23 genes

B

Differentially expressed probe sets matching known mammary involution genes*			
Probe Set ID	Fold, KO vs. WT	Gene Description	Gene Symbol
1417290_at	82.0	leucine-rich alpha-2-glycoprotein 1	Lrg1
1419075_s_at	40.6	serum amyloid A 1	Saa1
1449326_x_at	38.6	serum amyloid A 2	Saa2
1428572_at	38.1	brain abundant, membrane attached signal protein 1	Basp1
1416523_at	27.6	ribonuclease, RNase A family, 1 (pancreatic)	Rnase1
1452114_s_at	21.7	insulin-like growth factor binding protein 5	Igfbp5
1417130_s_at	14.7	angiopoietin-like 4	Angptl4
1420438_at	13.9	orosomucoid 2	Orm2
1417852_x_at	12.0	chloride channel calcium activated 1	Clca1
1417268_at	10.4	CD14 antigen	Cd14
1418283_at	10.4	claudin 4	Cldn4
1450826_a_at	7.7	serum amyloid A 3	Saa3
1416576_at	7.4	suppressor of cytokine signaling 3	Socs3
1455899_x_at	6.9	suppressor of cytokine signaling 3	Socs3
1448377_at	5.9	secretory leukocyte protease inhibitor	Slpi
1418021_at	5.4	complement component 4 (within H-2S)	C4
1451737_at	5.3	phosphatidylinositol 3-kinase, regulatory subunit, polypeptide 1 (p85 alpha)	Pik3r1
1417850_at	4.5	retinoblastoma 1	Rb1
1425249_a_at	4.3	TYRO3 protein tyrosine kinase 3	Tyro3
1425476_at	4.2	procollagen, type IV, alpha 5	Col4a5
1425475_at	3.5	procollagen, type IV, alpha 5	Col4a5
1417494_a_at	3.4	ceruloplasmin	Cp
1423233_at	3.4	CCAAT/enhancer binding protein (C/EBP), delta	Cebpd
1421752_a_at	3.3	serine (or cysteine) proteinase inhibitor, clade B, member 5	Serpinb5
1418981_at	3.1	caspase 12	Casp12
1455393_at	3.0	ceruloplasmin	Cp
1448734_at	3.0	ceruloplasmin	Cp
1417495_x_at	2.9	ceruloplasmin	Cp
1450355_a_at	2.8	capping protein (actin filament), gelsolin-like	Capg
1418374_at	2.7	FXYD domain-containing ion transport regulator 3	Fxyd3
1422438_at	2.6	epoxide hydrolase 1, microsomal	Ephx1
1448272_at	2.6	B-cell translocation gene 2, anti-proliferative	Btg2
1417455_at	2.5	transforming growth factor, beta 3	Tgfb3
1460243_at	2.5	serine palmitoyltransferase, long chain base subunit 2	Sptlc2
1417496_at	2.4	ceruloplasmin	Cp
1423456_at	2.2	basic leucine zipper and W2 domains 2	Bzw2
1450009_at	2.2	lactotransferrin	Ltf
1418364_a_at	2.2	ferritin light chain 1	Ftl1
1460700_at	2.2	signal transducer and activator of transcription 3	Stat3
1454758_a_at	2.1	transforming growth factor beta 1 induced transcript 4	Tgfb1i4
1426587_a_at	2.1	signal transducer and activator of transcription 3	Stat3
1460235_at	2.1	scavenger receptor class B, member 2	Scarb2
1451310_a_at	2.1	cathepsin L	Ctsl

* Known involution gene lists were compiled from Stein *et al.* 2004 and Clarkson *et al.* 2004.

FIG. 4—*Continued.*

involved in cellular metal ion homeostasis, 6 were differentially expressed. Among other selected biological processes that were significantly affected due to the absence of Mkl1, 8 of 85 muscle development genes, 10 of 195 cell motility transcripts, 14 of 345 cell death-associated genes, 6 of 86 homeostasis-associated transcripts, and 2 of 4 genes involved in nitric oxide-associated processes were differentially expressed in *Mkl1*$^{-/-}$ mammary glands (see Table S2 in the supplemental material).

A total of 48 genes (65 probe sets) were found to be significantly down-regulated (Fig. 4; see Table S1 in the supplemental material); among these genes, several previously demonstrated to be Srf transcriptional targets were identified. Of the 48 genes, upstream promoter sequences could be identified from database searches for 37 (42 probe sets). The Clover program (23) was used to scan a precompiled library of 542 vertebrate motifs from the TRANSFAC Professional database (46), version 8.3, against a 1-kb upstream promoter sequence of each of the 37 genes to identify significantly overrepresented motifs. Based on this analysis, sixteen of the 37 down-regulated genes contained one or more predicted Srf binding motifs in their promoter sequences (see Table S3 in the supplemental material). Of these 16 genes, 5 are known to be involved in muscle development and/or contraction and are previously identified Srf targets (actin alpha 1 in skeletal muscle, *Acta1*; actin alpha 2 in smooth muscle of aorta, *Acta2*; calponin 1, *Cnn1*; myosin heavy polypeptide 11 in smooth muscle, *Myh11*;

tropomyosin 2 beta, *Tpm2*). The other 11 genes are from a variety of putative or unknown functional classes (apolipoprotein D, *Apod*; Ets variant gene 6 [Tel oncogene], *Etv6*; heterogeneous nuclear ribonucleoprotein A/B, *Hnrpab*; disintegrin-like metalloprotease [reprolysin type] with thrombospondin type 1 motif, 5 [aggrecanase-2], *Adamts5*; ATP-binding cassette, subfamily E [OABP], member 1, *Abce1*; fatty acid desaturase 2, *Fads2*; cDNA sequence BC00398, Entrez gene 80295; beta-galactoside alpha 2,6 sialyltransferase 1, *St6gal1*; solute carrier family 25 [mitochondrial carrier, citrate transporter], member 1, *Slc25a1*; RIKEN cDNA F630022B06 gene, Entrez gene 239827; transmembrane protein 16D [eight membrane-spanning domains], *Tmem16d*); these 11 genes have not heretofore been implicated as possibly responsive to Srf in their transcriptional control (65, 83).

Involution-related genes, including those of the Stat3 pathway, are up-regulated in postpartum *Mkl1*$^{-/-}$ mammary glands. Mammary epithelial cells pass through a well-choreographed series of developmental stages during pregnancy and the postpartum period. During mammary gland development, the switches from proliferation to differentiation to secretion, and then to cell death and remodeling, are precisely controlled; consistent with their uniqueness, each of these stages is associated with a specific gene expression profile (18). Recent microarray analyses showed the involution process to involve a transient increase in the expression of components of the death receptor apoptosis pathways, including various Tnf superfamily genes, proinflammatory cytokines, and acute-phase response genes during the first day after weaning, followed by induction of markers of phagocyte activity, matrix proteases, suppressors of neutrophils, soluble components of specific and innate immunity, and components of the mitochondrial/intrinsic apoptotic death pathway (18, 71).

Stat3 pathway signaling appears to be especially important for the normal involution process as demonstrated by conditional deletion of *Stat3* in differentiated mammary epithelium, which results in a decrease in apoptosis-induced remodeling and a marked delay in the onset of involution, with large alveolar structures, open lumina, and evidence of milk secretion remaining long after the cessation of suckling (16, 31, 32, 66). Stat3 functions during involution both to induce apoptosis of milk-producing cells and to mediate, in part, the expression of the immunity-related genes that are associated with postlactational regression. The induction of apoptotic cell death by Stat3 involves a recently described mechanism in which the phosphatidylinositol 3-kinase regulatory subunits p55alpha and p50alpha—which are expressed from different promoters of the *Pk3r1* gene, itself a direct transcriptional target of Stat3—are overexpressed and inhibit Akt/PKB survival signaling (1). The ability of Stat3 to regulate immunity-related gene expression is partially dependent upon cooperative binding with CAAT-enhancer binding proteins, including C/EBPdelta (which is also a transcriptional target of Stat3 in vivo), to specific sites in the gene promoters; thus, both Stat3 and C/EBPdelta are substantively involved in the acute-phase responses that occur during involution (2, 12, 32, 61).

A detailed analysis of the data from our microarray profiling of day 5 postpartum *Mkl1*$^{-/-}$ and wild-type mammary gland tissues revealed a strong statistical relationship between the observed alterations in gene expression and genes associated with involution. Of the 182 differentially expressed genes, 36 had been previously described as involution-related (18, 71) (Fig. 4B). The functional classification of these "involution signature genes" revealed that nine of them were either directly associated with acute-phase responses or induced by lipopolysaccharide, including *Stat3*, the C/EBPdelta gene, the monocyte differentiation antigen gene *CD14*, the ceruloplasmin gene (*CP*), and the genes for alpha(1)-acid glycoprotein 1 and 2 (orosomucoid 1 and 2 [*Orm1* and *Orm2*]) and serum amyloids A1, A2, and A3 (*Saa1*, *Saa2*, and *Saa3*).

In addition, three Stat3 pathway-associated genes (*Socs3*, *Igfbp5*, and *Slpi*)—all recently implicated in mammary gland involution—were significantly up-regulated in *Mkl1*$^{-/-}$ postpartum mammary tissue. The genes encoding suppressor of cytokine signaling 3 (Socs3) protein is up-regulated and is a direct transcriptional target of Stat3 in involuting mammary gland (5, 6). Socs3 inhibits leukemia inhibitory factor (Lif)-induced phosphorylation of Jak2, gp130, and Stat3 in mammary epithelium and thus terminates the signaling of multiple cytokines (for example, prolactin); in addition, Socs3 inhibits the Lif-induced expression by the pituitary gland of proopiomelanocortin and adrenocorticotropic harmone, both of which are critical for normal mammary gland physiology (6). Insulin-like growth factor binding protein 5 (Igfbp5) is also a target for Stat3 during involution (16) and its induction at the onset of the second phase of normal involution promotes apoptosis within the mammary gland due to interference with IGF1R survival signaling (14–16, 74). Secretory leukocyte protease inhibitor (Slpi), a potent inhibitor of neutrophil proteases (68) that is encoded by a Stat3-induced gene, is markedly up-regulated during normal involution of the mammary gland, presumably serving to physiologically dampen the immune responses that accompany the involution process (18).

To expand upon these microarray data, we compared the expression temporally during the reproductive cycle of several involution-related genes (*C/EBPdelta*, *Clca1*, *Clca2*, *Igfbp5*, *Lrg1*, *Saa2*, *Stat3*, and *Tyro3*) between *Mkl1*$^{-/-}$ and wild-type mammary glands using real-time PCR analysis (Fig. 5). Total RNAs were extracted from the mouse mammary glands at several stages during the reproductive cycle (the virgin stage, days 13 and 19 of pregnancy, postpartum days 5 and 10, and—for wild-type mice only—days 2 and 3 of normal involution), and the levels of expression of the various mRNAs were examined. As shown in Fig. 5, the expression of these involution-related genes was aberrantly up-regulated as early as day 19 of pregnancy in *Mkl1*$^{-/-}$ mammary glands to levels at, or above, those normally associated with mammary tissue at day 3 of involution after weaning, suggesting premature involution. The expression of these genes increased yet further in *Mkl1*$^{-/-}$ mammary glands at postpartum days 5 and 10—despite active suckling by pups—to levels that equaled, or in some cases substantially exceeded, those observed in wild-type mammary glands at day 2 or 3 of normal postweaning involution. Taken as a whole, these data indicate that the absence of Mkl1 is associated with a mammary gland transcriptional profile consistent with an early onset of the involution process normally observed after weaning, which begins even during pregnancy and becomes progressively more pronounced in the postpartum period.

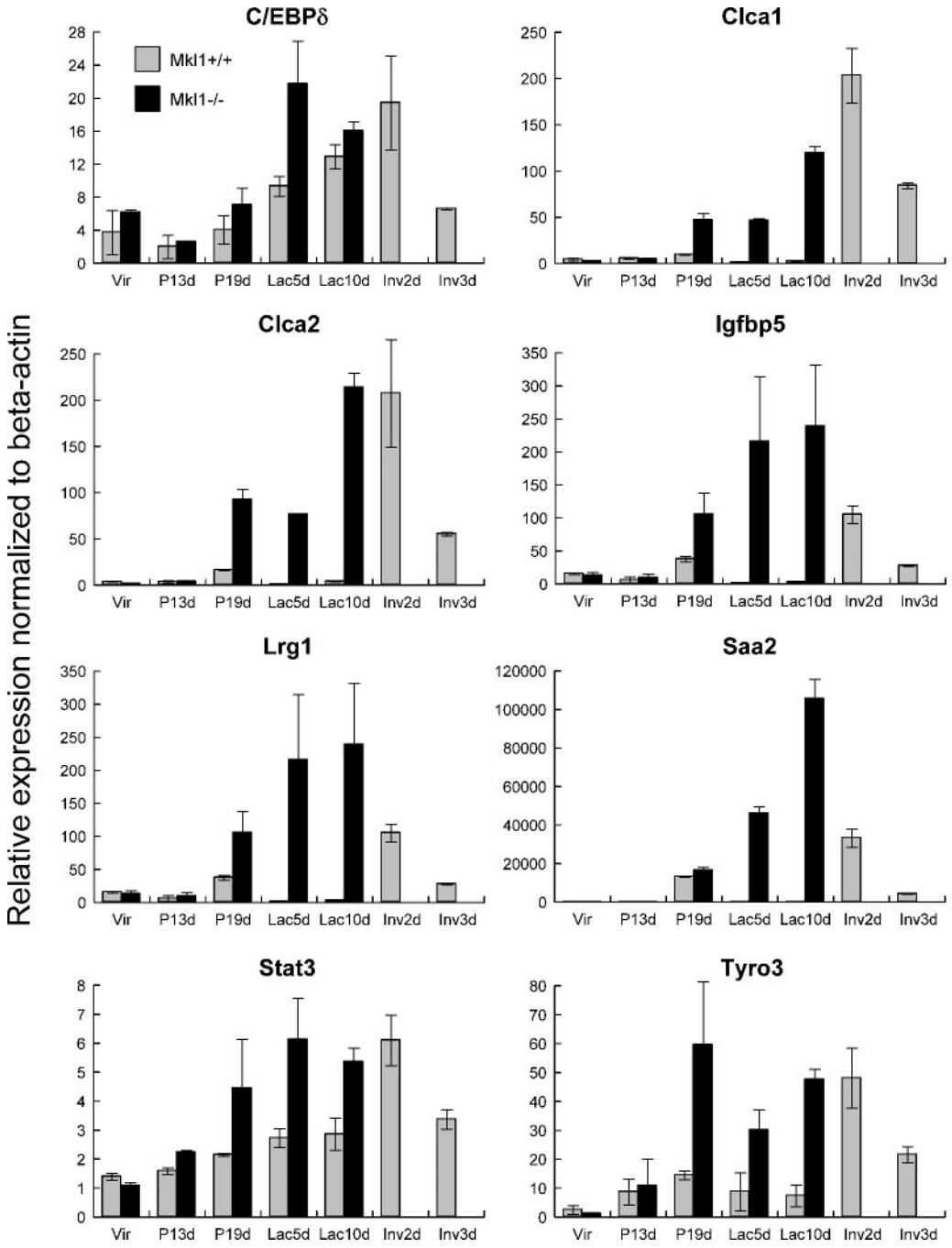

FIG. 5. Absence of Mkl1 is associated with a gene transcription profile indicative of aberrant, premature mammary gland involution. Real-time PCR quantitation of the expression of selected involution genes in *Mkl1*$^{-/-}$ and *Mkl1*$^{+/+}$ mammary glands is illustrated. Total RNAs were extracted and analyzed from *Mkl1*$^{-/-}$ (−/−) and wild-type (+/+) mammary glands from virgin (5-week-old [Vir]), 13-day-pregnant (P13d), 19-day-pregnant (P19d), 5-day-postpartum (Lac5d), and 10-day-postpartum (Lac10d) females. In addition, mammary tissue was collected at day 2 (Inv2d) and day 3 (Inv3d) of involution, and total RNAs were extracted from wild-type females following removal of suckling pups. *C/EBPdelta*, *Clca1* (chloride channel calcium activated 1) and *Clca2*, *Igfbp5*, *Lrg1* (leucine-rich alpha-2-glycoprotein 1), *Saa2*, *Stat3* (signal transducer and activator of transcription 3), and *Tyro3* (protein tyrosine kinase 3) mRNA levels were analyzed with real-time PCR and normalized to beta-actin gene transcription levels. The data shown are from three independent experiments; error bars indicate standard deviations. Note that the expression of these genes, which normally occurs at substantial levels only during the involution of mammary gland tissue, begins at least as early as day 19 of pregnancy and is sustained throughout the immediate postpartum period in *Mkl1*$^{-/-}$ females.

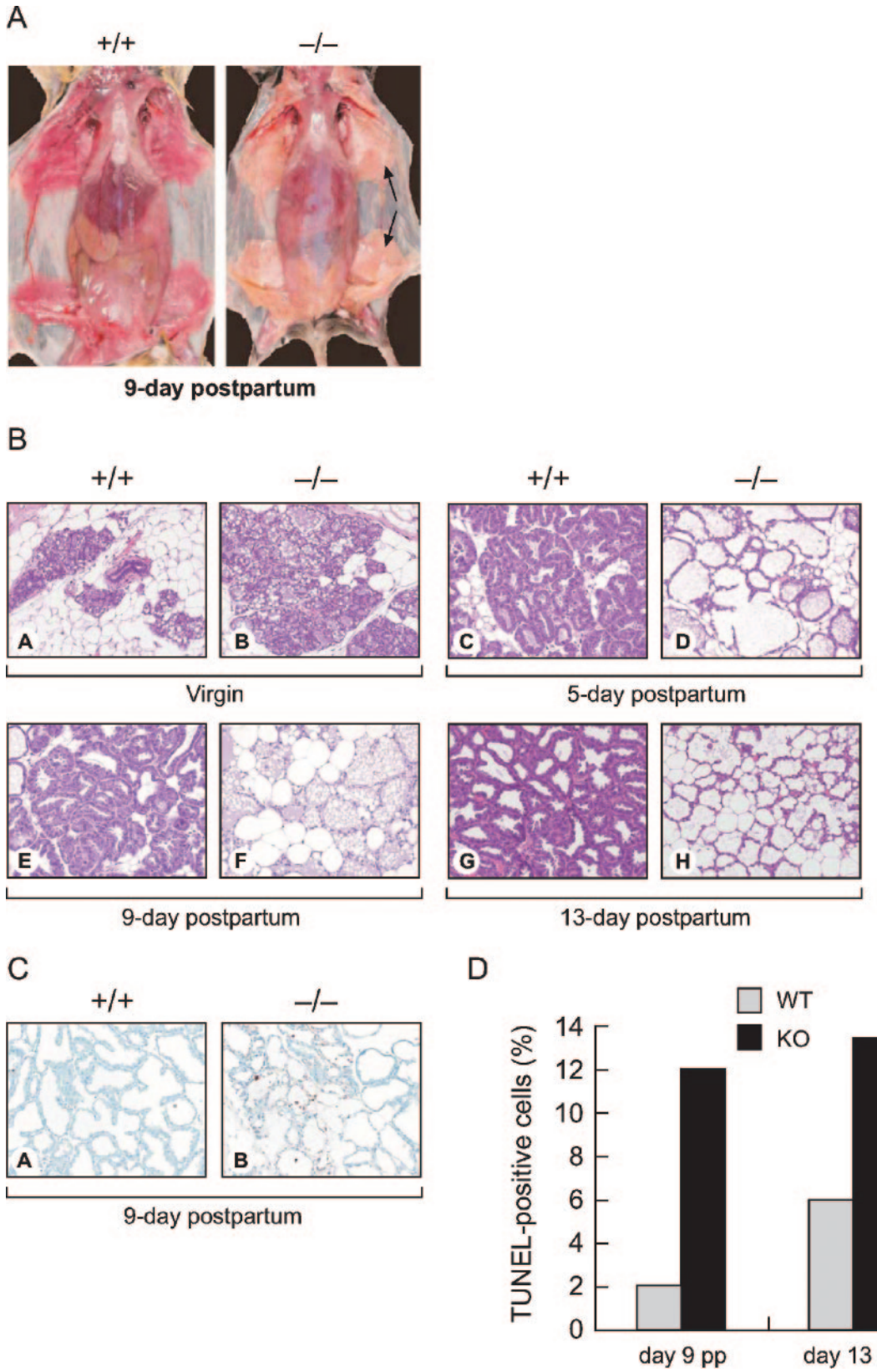

FIG. 6. Gross and histological analysis of mammary glands from *Mkl1*$^{-/-}$ female mice. (A) Gross appearance of mammary gland tissues from *Mkl1*$^{-/-}$ dams at postpartum day 9. The mammary tissue in the subcutaneous space is indicated unilaterally (arrows) on the image of the *Mkl1*$^{-/-}$ female. Note the pallor of the mammary glands of the *Mkl1*$^{-/-}$ mouse compared to the tissue from a wild-type animal as shown in panel B. (B) Hematoxylin and eosin-stained virgin and postpartum mammary gland sections. Note the progressive increase in fat tissue and decrease in the

Milk accumulation and premature onset of histological involution-like changes in *Mkl1*$^{-/-}$ mammary glands. To confirm our findings from microarray and real-time PCR analyses, we next investigated the gross and histological appearance of *Mkl1*$^{-/-}$ mammary tissue. The gross appearance of *Mkl1*$^{-/-}$ and wild-type mammary glands at postpartum day 9 showed a loss of the normal reddish-pink color of the tissues in *Mkl1*$^{-/-}$ mice, their appearance being characterized instead by a light yellow-tan color (Fig. 6A). The overall abundance of the mammary tissues was similar, or even increased, in the *Mkl1*$^{-/-}$ mice compared to that in their wild-type counterparts, which is indicative of the accumulation of milk due to inefficient let-down.

The differences were more apparent in histological sections (Fig. 6B). The lumina of the mammary alveoli were full of milk and became dilated in the *Mkl1*$^{-/-}$ glands in the initial postpartum period (e.g., postpartum day 5) (Fig. 6B, panel D). The alveolar epithelium was flattened compared with the epithelial cells in the wild-type mammary gland, which ranged from plump and cubical to low columnar with abundant cytoplasm (Fig. 6B, compare wild-type glandular tissues shown in panels C, E, and G with *Mkl1*$^{-/-}$ glands shown in panels D, F, and H). The postpartum mammary glands of *Mkl1*$^{-/-}$ females had markedly increased adipose tissue (Fig. 6B, panels D, F, and H), which was more suggestive of the normal histological appearance of a gland undergoing postweaning involution than normal lactating mammary tissue. A progressive loss of epithelial cell components and an increase of adipose tissue were noted at postpartum days 9 and 13 in the mammary glands of the *Mkl1*$^{-/-}$ mice (Fig. 6B, panels F and H). In addition to these changes, the histological analysis also indicated a milk accumulation in the lumina of the alveoli in *Mkl1*$^{-/-}$ mammary glands during the postpartum period (Fig. 6B, panels D, F, and H). In contrast to the marked alterations observed in *Mkl1*$^{-/-}$ and wild-type mammary tissues postpartum, the histology of the mammary glands of virgin mice was not substantively different (Fig. 6B, panels A and B).

It has been reported that local stimulation (e.g., by milk accumulation in the alveoli) can induce mammary gland epithelial cell apoptosis and involution (25, 45). Although the causes are likely multifactorial, the premature onset of involution and cell death in *Mkl1*$^{-/-}$ mammary glands may occur in part due to this mechanism, as well as to the absence of anti-apoptotic effects mediated by Mkl1 (63). To determine whether the abnormalities we observed in postpartum *Mkl1*$^{-/-}$ mammary tissues were accompanied by increased apoptotic cell death, we performed in situ TUNEL assays (Fig. 6C). Quantitation of TUNEL-positive cells showed comparable numbers of apoptotic cells in virgin and 5-day-postpartum *Mkl1*$^{-/-}$ and wild-type mammary glands (data not shown) but a marked increase in apoptotic cell death at postpartum days 9 and 13 in the *Mkl1*$^{-/-}$ glands (Fig. 6C and D).

The gross and histological changes observed in *Mkl1*$^{-/-}$ mammary tissue are consistent with the alterations in global mammary gland gene expression that we identified, i.e., both indicate that Mkl1 function is essential for the sustained functional integrity of mammary tissue required to support normal lactation. Although milk production takes place during the early postpartum period in *Mkl1*$^{-/-}$ mammary glands, the premature onset of an involution-like process precludes sustained lactation beyond the first week postpartum.

Dysfunctional myoepithelial cells in *Mkl1*$^{-/-}$ mammary tissue. There are two types of epithelial cell layers in the mammary gland: the luminal epithelial layer, which is comprised of the milk-secreting cells, and the basal myoepithelial cell layer, which responds to suckling stimuli with oxytocin-induced contraction and milk ejection (40). Differentiated myoepithelial cells contain large amounts of microfilaments, dense plaques (cell-matrix adherence junctions characteristic of smooth muscle cells) and smooth muscle cytoskeletal and contractile proteins, such as smooth muscle calponin (Cnn1) and the smooth muscle myosin heavy chain (Myh11) (60). As noted, Mkl1 binds stably to Srf and is known to strongly activate a number of smooth muscle genes (13, 65, 78). Furthermore, overexpression of Mkl1 can activate smooth muscle-specific genes in several nonmuscle cell lines (13, 17, 20).

Consistent with these findings, our microarray analysis of whole mammary tissues demonstrated significant down-regulation of a group of muscle development- and differentiation-associated genes in *Mkl1*$^{-/-}$ mammary glands (Fig. 4; see Tables S1 and S2 in the supplemental material). These data suggested that Mkl1 may play a role in the regulation of smooth muscle gene expression in the mammary gland, including particularly the myoepithelial cells, with the absence of the protein impairing normal glandular function and myoepithelial cell responses. To further examine this possibility, we first determined specifically the expression of *Mkl1* in mammary tissue throughout the normal reproductive cycle. Real-time PCR analysis using total RNA prepared from mammary glands of wild-type virgin mice, as well as wild-type mice at days 13 and 19 of pregnancy, postpartum-lactation days 5 and 10, and days 2 and 3 of involution, showed Mkl1 to be expressed at all stages, the highest levels being found in virgin and early-involution mammary glands (Fig. 7A). Next, we examined specifically the expression of *Mkl1* in the myoepithelial cells, using RNA prepared from cells purified to homogeneity from day 5 postpartum lactating *Mkl1*$^{-/-}$ and wild-type mammary glands. As shown in Fig. 7B (left panel), *Mkl1* expression was more than 50-fold higher in myoepithelial cells compared to day 5 postpartum whole mammary tissue. No significant expression

epithelial cell component of the *Mkl1*$^{-/-}$ glands (D, F, and H) compared to the wild-type glands (C, E, and G). (C) TUNEL assay for identification of apoptotic cells in mammary gland sections from 9-day-postpartum mice; note that the *Mkl1*$^{-/-}$ mammary tissues show markedly increased numbers of cells undergoing apoptotic death (indicated by brown staining) compared to the wild-type mammary tissue. (D) Quantitative assessment of apoptosis in mammary tissues at postpartum days 9 and 13. A total of 500 epithelial cells from typical histological sections (such as those shown in panel C) were counted in each of three independent determinations; the data shown are representative of one such determination. WT, wild type; KO, knockout.

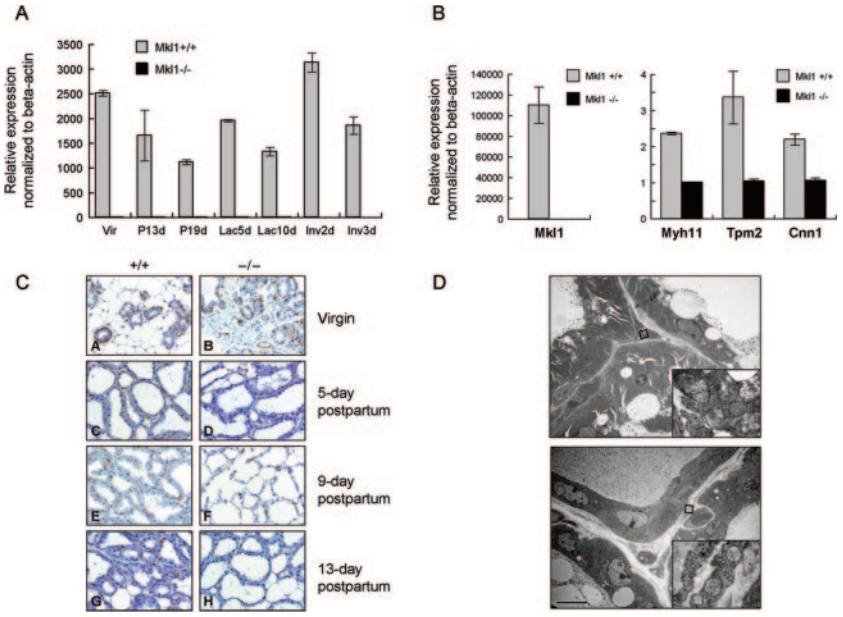

FIG. 7. Muscle-specific gene expression is markedly reduced in *Mkl1*$^{-/-}$ mammary glands. (A) Total RNAs were extracted from *Mkl1*$^{+/+}$ and *Mkl1*$^{-/-}$ mammary glands at the indicated times during the reproductive cycle, and expression of *Mkl1* mRNA was analyzed using real-time PCR and normalized to beta-actin levels. The data illustrated are from three independent experiments; error bars indicate standard deviations. Vir, virgin mice; P13d, 13-day-pregnant mice; P19d, 19-day-pregnant mice; Lac5d, 5-day-postpartum mice; Lac10d, 10-day-postpartum mice; Inv2d, mice at day 2 of involution; Inv3d, mice at day 3 of involution. (B) Myoepithelial cells were isolated from day 5 postpartum mammary glands of *Mkl1*$^{-/-}$ and wild-type females, and total RNAs were extracted. The expression levels of the mRNAs for *Mkl1* (left panel), *Myh11*, *Tpm2*, and *Cnn1* (left panel) were quantified using real-time PCR analysis and normalized to beta-actin transcription levels. Note that the normal level of *Mkl1* transcription is very high (~60-fold) in the myoepithelial cells (B, left panel) compared to the mammary gland tissue as a whole (panel A, Lac5d). (C) SMA staining of the myoepithelial cells of *Mkl1*$^{-/-}$ and wild-type mammary glands is markedly diminished in the tissues lacking Mkl1. (D) Myoepithelial cells from *Mkl1*$^{-/-}$ (lower panel) and wild-type (upper panel) mammary glands were examined by electron microscopy. Boxes overlie the myoepithelial cells and represent areas shown in higher magnification to demonstrate the abnormal morphology of the mitochondria in the *Mkl1*$^{-/-}$ cells, which is similar to that observed in *Mkl1*$^{-/-}$ cardiac muscle (Fig. 2B).

of *Mkl1* was detected by real-time PCR in either whole mammary gland tissue (Fig. 7A) or purified myoepithelial cells (Fig. 7B, left panel) from *Mkl1*$^{-/-}$ mice.

The profound abnormalities that we identified in *Mkl1*$^{-/-}$ mammary gland morphology and function suggest the absence of substantive functional complementation by either myocardin or Mkl2. Although myocardin gene expression was not detected in purified myoepithelial cells from either wild-type or *Mkl1*$^{-/-}$ mammary tissues by real-time PCR, *Mkl2* was present in these cells in both normal and *Mkl1*$^{-/-}$ mice; indeed, expression of *Mkl2* was found to be marginally (1.44-fold) elevated in *Mkl1*$^{-/-}$ myoepithelial cells compared to wild-type myoepithelial cells (data not shown). These findings suggest that Mkl1 plays a dominant role compared to myocardin and Mkl2 in normal mammary gland physiology, especially with respect to myoepithelial cell function.

To more fully understand the consequences of Mkl1 absence on the mammary myoepithelial cells, we examined a myoepithelial cell differentiation marker, SMA—a direct Srf transcriptional target known to be regulated by, but not solely dependent upon, coactivation mediated via myocardin in cardiac and certain smooth muscle cells (38)—in wild-type and *Mkl1*$^{-/-}$ mammary glands by immunohistochemical analysis. As seen in Fig. 7C (panels A, C, E, and G), normal myoepithelial cells stain for SMA at their location in the basal layer surrounding each alveolus. In contrast to the essentially continuous, single-cell layer of myoepithelial cells surrounding the alveoli of normal mammary glands, in the *Mkl1*$^{-/-}$ mammary tissues, the myoepithelium was discontinuous and the SMA staining was significantly less intense; these findings were especially evident in postpartum *Mkl1*$^{-/-}$ mammary tissue sections (Fig. 7C, panels D, F, and H) and were apparent even in the few areas of *Mkl1*$^{-/-}$ glands that were otherwise more or less structurally intact (e.g., Fig. 7C, panel H, shows a day 13 postpartum *Mkl1*$^{-/-}$ histological section with only modest loss of overall structural integrity).

To further quantify the effect of Mkl1 absence on the mammary myoepithelial cells, we assessed the mRNA levels of several differentiation markers in purified myoepithelial cells from day 5 postpartum lactating *Mkl1*$^{-/-}$ and wild-type mammary glands. These markers—*Myh11*, *Cnn1*, and *Tpm2*—are all known to be dependent upon Srf for their transcriptional activation (21, 43, 44, 53). Although a very low level of expression of each of these three genes was evident by real-time PCR in *Mkl1*$^{-/-}$ myoepithelial cells, each was expressed at an approximately 2.5- to 3-fold lower level compared to wild-type cells (Fig. 7B, right panel). We also examined CD10/neutral endopeptidase 24.11, a marker also found on B lymphocytes but specific within mammary tissue for the myoepithelial cells (4, 22, 29, 42, 57, 62), the expression of which is not known to be affected by Srf. Interestingly, CD10 was significantly up-regulated in the *Mkl1*$^{-/-}$ myoepithelial cells (data not shown); the impact of this up-regulation on the differentiation and

function of the myoepithelial cells is unknown. Overall, these data, which are consistent with our expression profiling results on whole mammary gland tissue (Fig. 4), suggest that the normal myoepithelial cell functional program is disrupted by the loss of Mkl1.

Ultrastructural examination of the mammary myoepithelial cells from day 13 postpartum *Mkl1*$^{-/-}$ and wild-type mice by electron microscopy revealed an overall dysmorphic appearance of the *Mkl1*$^{-/-}$ cells, which were shrunken and discontinuous compared to the cells from wild-type tissue (Fig. 7D). The most obvious organellar abnormality seen in the *Mkl1*$^{-/-}$ myoepithelial cells involved the mitochondria (Fig. 7D, insets), which were swollen and had lost their normal crystal structures in a pattern very similar to that observed in *Mkl1*$^{-/-}$ embryonic myocardium (Fig. 2B, panels C and D). While is not clear whether these defects represent a primary mitochondrial abnormality due to Mkl1 absence or reflect a more global cellular dysfunctional state, our microarray analysis of whole mammary tissue did reveal possible deregulation of acetyl-CoA metabolism that could potentially impact mitochondrial function. For example, expression of the ATP citrate lyase (*Acly*) gene, which encodes a protein that generates cytosolic acetyl-CoA from mitochondrion-derived citrate (9, 10), was decreased twofold; expression of the gene encoding the solute carrier family 25 member 1 protein (*Slc25a1*)—a mitochondrial carrier protein that transports citrate across the inner mitochondrial membrane (58)—was decreased 2.7-fold in Mkl1$^{-/-}$ mammary tissues compared to wild-type glands (interestingly, we identified a potential motif for Srf DNA binding in the *Slc25a1* promoter sequences [see Table S3 in the supplemental material], suggesting that the gene might be a heretofore unrecognized Srf transcriptional target); and the *Nudt7* gene, which encodes a peroxisomal hydrolase specific for coenzyme A (26) was up-regulated slightly more than twofold. Additional studies will be required to elucidate the exact metabolic functions deregulated due to the lack of Mkl1, as well as the manner by which Acly, Nudt7, Slc25a1m, and other mitochondrion-associated proteins (see Table S4 in the supplemental material) are aberrantly expressed in *Mkl1*$^{-/-}$ mammary tissue and might contribute to cellular dysfunction. Nonetheless, taken as a whole, these findings indicate that the lack of Mkl1 is not compatible with normal mammary myoepithelial cell function and suggest that mitochondrial dysfunction could possibly be one consequence of Mkl1 absence.

DISCUSSION

To study the functions of *Mkl1* in mammalian development, we generated knockout mice that lack the gene. Our data demonstrate an essential function for Mkl1 in the female reproductive cycle; specifically, the lack of Mkl1 abrogates physiologic mammary gland function during the postpartum lactation period, an effect associated with the onset of a premature involution-like phenotype in females that are actively suckling pups, as well as an impairment of the mammary myoepithelial cells that normally function in the oxytocin-mediated milk ejection response. These defects result in an inability of *Mkl1*$^{-/-}$ dams to support the nutritional requirements of suckling pups and the death of these pups within the initial 14 to 17 days of life independent of their *Mkl1* genotype.

In addition to the absolute requirement of Mkl1 for normal mammary gland function, Mkl1 appears to be conditionally required for the integrity of the myocardial cells during embryonic development, with approximately 40% of *Mkl1*$^{-/-}$ mouse embryos suffering lethal cardiac cell necrosis at approximately embryonic day 10.5. Although this result is not unexpected in light of the well-known importance of Srf function during heart development (49, 77), we are uncertain as to the reason(s) for the incomplete penetrance of this cardiac phenotype. Background strain variations from generation to generation of our mice could potentially affect the penetrance of the phenotype, given that these knockout animals are still on a mixed 129Sv × C57BL/6 background at the time of this publication. Notably, however, independently generated Mkl1 (Mrtf-a) knockout mice, also on a mixed 129 × C57BL/6 background, have not been observed to develop any cardiac abnormalities during embryogenesis or in adulthood, although they possess mammary gland dysfunction essentially identical to that described in this report (37a). This observation suggests that, rather than due to genetic strain background differences, the unknown factor(s) that predisposes only a subset of our embryos to death may reflect an inability of Mkl1$^{-/-}$ cardiomyocytes to correctly respond to selected (and variably present) environmental stresses during development.

Rather than apoptosis or autophagy, we observed a necrosis-like death of *Mkl1*$^{-/-}$ cardiac cells in our mouse embryos. Coincident with this necrotic cell death, we identified ultrastructural evidence of myocardial cell (as well as mammary myoepithelial cell) mitochondrial dysfunction. Mkl1 has previously been shown to modulate apoptotic cell death, overexpression of the protein partially inhibiting tumor necrosis factor-induced apoptosis with attendant inhibition of caspase activation (63). Although establishment of a cause-effect relationship between the mitochondrial abnormalities in *Mkl1*$^{-/-}$ cells and the death of these cells by necrosis will require further analyses, recent studies show that mitochondrial function clearly plays a role in modulating not only apoptotic but also necrotic cell death—the latter being induced by such stimuli as reactive oxygen species-mediated cellular damage or Ca^{2+} overload (8, 52). Reactive oxygen species and Ca^{2+} overload are known to be key factors involved in necrotic injury of cardiocytes by experimentally induced ischemia/reperfusion (a process that mimics myocardial infarction) (81); normal Mkl1 function may therefore serve as a protectant against ischemia-induced cardiac cell death.

Interestingly, our analysis of the hematopoietic system of *Mkl1*$^{-/-}$ mice failed to identify any clear-cut abnormalities—including of the megakaryocyte/platelet lineage—despite the expression of the gene in mature megakaryocytes (S. W. Morris, unpublished data) and the fact that *MKL1* was initially identified due to its involvement in the *RBM15-MKL1* fusion generated by the t(1;22) chromosomal translocation specific to pediatric acute megakaryoblastic leukemias (41, 48). Thus, while aberrant expression of the gene appears to contribute to leukemogenesis, its normal function is not essential for hematopoiesis.

A recent study in which the *Drosophila Mkl1* counterpart (*CG32296*, also known as *mal-d*) was interrupted revealed absence of the gene to cause early larval lethality and to be essential for the accumulation of a robust actin cytoskeleton

during the cellular migration processes required for normal development (69). Given the widespread expression of *Mkl1* and the role of the gene in mediating the TCF-independent activation of subsets of muscle, immediate-early, and cytoskeletal Srf target genes, we had anticipated that more profound phenotypic abnormalities would accompany mammalian *Mkl1* deletion. However, since myocardin and Mkl2 are coexpressed with Mkl1 in certain muscle tissues, and Mkl-1 and -2 are both present in other nonmuscle sites, it is likely that Mkl1 function is frequently redundant with the other two myocardin/MKL family members. Likewise, it is probable that TCF-dependent activation of a subset of Srf target genes may substitute for myocardin/MKL-dependent transcription of these genes in certain tissues, or under various growth or differentiation conditions. Future studies in which two or all three myocardin/Mkl factors are deleted in vivo will be required to address these issues.

Mkl1 is not required for muscle cell development. The three members of the myocardin/MKL transcription factor family (myocardin, Mkl1, and Mkl2) physically associate with Srf and function to coactivate transcription from promoters with Srf binding sites (13, 50, 63, 78). Such Srf binding sites (CArG boxes) have been identified in the transcriptional regulatory elements of various muscle-restricted or -important genes (49, 59, 77, 79). *Mkl1* is widely expressed, including in heart, skeletal, and smooth muscle tissues (20, 41, 48, 63, 78). *Mkl2*, on the other hand, exhibits a more restricted spatial-temporal tissue expression pattern (37, 56, 64, 78); for example, expression of *Mkl2* during embryogenesis is restricted mainly to the developing rhombomeres of the brain, the heart, and the aortic arch and branchial arch arteries (37). Previous studies have suggested critical roles for the two genes in muscle development and function; for example, it has been shown that Mkl1/2 activity is required for the differentiation of C2C12 cells, a skeletal myogenic cell line (64). In addition, enforced expression of Mkl1 and Srf in undifferentiated Srf-deficient embryonic stem cells induces a smooth muscle phenotype and activates multiple endogenous smooth muscle cell-restricted genes (20). In contrast to the widespread expression of *Mkl-1* and *-2*, myocardin is expressed only in heart and smooth muscle tissues (76) and is known to play an essential role in smooth muscle cell development since myocardin knockout mice die by day E11.5 from a lack of vascular smooth muscle cells; interestingly, however, myocardin absence did not perturb heart development in these knockout mice despite its robust cardiac expression during embryogenesis (38). Similarly, Mkl2 function appears to be especially important during embryogenesis for smooth muscle differentiation in the developing cardiac outflow tracts, as well as during the development of the ventricular septa, with mice that harbor a conditional insertional mutation of the gene dying between E17.5 and postnatal day 1 from defects at these sites; however, although Mkl2 absence is associated with a greater degree of cardiac abnormalities than myocardin null mice, the development of the myocardium proper in *Mkl2*$^{-/-}$ animals appears to be relatively intact, with only a thinning of the myocardial wall being noted (37, 56). As a whole, these data indicate that myocardin/MKL transcription factor family members play important roles in muscle tissue development; however, the results reported herein indicate that Mkl1 alone is not essential for muscle development, perhaps due to redundant function with myocardin and Mkl2.

Deletion of Mkl1 impairs mammary myoepithelial cell function and is associated with premature mammary involution, resulting in failure of lactation. Unlike mice lacking either myocardin or Mkl2 (37, 38, 56), *Mkl1*$^{-/-}$ mice can be viably born and survive to adulthood, allowing us to determine the unique, nonredundant postnatal functions of the protein without the necessity of conditional-deletion experimental approaches. Despite broad *Mkl1* tissue expression in adult organs (20, 41, 48, 63, 78), mice lacking the gene that were viably born had a normal life span, suffered no apparent phenotypic abnormalities (other than the observed mammary gland dysfunction), and possessed normal fertility. From both a basic biological as well as a pragmatic viewpoint, the minimal phenotypic consequences of Mkl1 absence in the whole postnatal organism are of interest. Our prior studies have shown the leukemia-associated RBM15-MKL1 fusion protein to exhibit a marked gain of function with respect to its ability to activate SRF-dependent gene transcription compared to normal MKL1 transcriptional activation capability (13). Inhibition of this gain-of-function feature of the chimeric leukemia oncoprotein would be predicted to be of therapeutic benefit, and the absence of severe abnormalities due to the lack of Mkl1 suggests that future therapeutic approaches that might be designed to inhibit aberrant MKL1 function in the leukemia-associated chimera would not be associated with undue toxicity due to concomitant impairment of normal MKL1 activity.

The factors controlling the physiological mammary gland involution that occurs after weaning are poorly understood; further, the mechanisms by which the involution process itself takes place have only recently been examined using modern molecular biology techniques (18, 71). Our data indicate that normal Mkl1 function (and presumably by extension, normal Srf function as well, although this is not yet proven) is absolutely required to prepare and maintain the mammary gland for physiologic lactation. The specific Mkl1 transcriptional target genes required for normal mammary gland function are not known. Examination of our microarray data from postpartum day 5 mammary tissue revealed only four genes that were completely absent from Mkl1$^{-/-}$, but expressed in wild-type, mammary glands (see Table S5 in the supplemental material); only one of these genes (*CnnI*) has previously been implicated as playing a role in normal mammary gland physiology.

It is interesting to speculate that Mkl1 might serve as a master control switch that functions to regulate the normal onset of involution. Should this be the case, a number of cues would undoubtedly be expected to lie upstream to regulate Mkl1 itself, but one such Mkl1 regulatory factor could be increased intraglandular alveolar tension induced by milk retention in the mammary glands during the immediate postweaning period (25, 45). Both mammalian and *Drosophila* Mkl1 can be activated by mechanical cellular tension and its accompanying alterations of the actin cytoskeleton (50, 69); in addition, targeted mammary gland expression of constitutive Rho GTPase activity has recently been demonstrated to cause incomplete involution after weaning, thus implicating the Rho signaling pathway in the normal regulation of the involution process (36). Future studies in which Mkl1 is conditionally and uniquely overexpressed in the mammary glands, or Srf is con-

ditionally inactivated or overexpressed specifically in mammary tissue, should help to clarify these possibilities.

ACKNOWLEDGMENTS

We thank S. Li and Eric Olson (Department of Molecular Biology, University of Texas Southwestern Medical Center, Dallas) for sharing data prior to publication. Xiaoli Cui provided excellent experimental assistance.

This work was supported by National Institutes of Health grant CA 87064 to S.W.M., National Institutes of Health Cancer Center CORE grant 21765, and the American Lebanese Syrian Associated Charities, St. Jude Children's Research Hospital. G.W.R., L.H., and J.M.S. were supported by the Intramural Program of NIDDK, NIH.

REFERENCES

1. **Abell, K., A. Bilancio, R. W. Clarkson, P. G. Tiffen, A. I. Altaparmakov, T. G. Burdon, T. Asano, B. Vanhaesebroeck, and C. J. Watson.** 2005. Stat3-induced apoptosis requires a molecular switch in PI(3)K subunit composition. Nat. Cell Biol. **7:**392–398.
2. **Alam, T., M. R. An, and J. Papaconstantinou.** 1992. Differential expression of three C/EBP isoforms in multiple tissues during the acute phase response. J. Biol. Chem. **267:**5021–5024.
3. **Ashburner, M., C. A. Ball, J. A. Blake, D. Botstein, H. Butler, J. M. Cherry, A. P. Davis, K. Dolinski, S. S. Dwight, J. T. Eppig, M. A. Harris, D. P. Hill, L. Issel-Tarver, A. Kasarskis, S. Lewis, J. C. Matese, J. E. Richardson, M. Ringwald, G. M. Rubin, and G. Sherlock.** 2000. Gene ontology: tool for the unification of biology. The Gene Ontology Consortium. Nat. Genet. **25:**25–29.
4. **Atherton, A. J., M. J. O'Hare, L. Buluwela, J. Titley, P. Monaghan, H. F. Paterson, M. J. Warburton, and B. A. Gusterson.** 1994. Ectoenzyme regulation by phenotypically distinct fibroblast sub-populations isolated from the human mammary gland. J. Cell Sci. **107:**2931–2939.
5. **Auernhammer, C. J., C. Bousquet, and S. Melmed.** 1999. Autoregulation of pituitary corticotroph SOCS-3 expression: characterization of the murine SOCS-3 promoter. Proc. Natl. Acad. Sci. USA **96:**6964–6969.
6. **Auernhammer, C. J., and S. Melmed.** 2001. The central role of SOCS-3 in integrating the neuro-immunoendocrine interface. J. Clin. Investig. **108:**1735–1740.
7. **Baehrecke, E. H.** 2005. Autophagy: dual roles in life and death? Nat. Rev. Mol. Cell Biol. **6:**505–510.
8. **Baines, C. P., R. A. Kaiser, N. H. Purcell, N. S. Blair, H. Osinska, M. A. Hambleton, E. W. Brunskill, M. R. Sayen, R. A. Gottlieb, G. W. Dorn, J. Robbins, and J. D. Molkentin.** 2005. Loss of cyclophilin D reveals a critical role for mitochondrial permeability transition in cell death. Nature **434:**658–662.
9. **Bauer, D. E., G. Hatzivassiliou, F. Zhao, C. Andreadis, and C. B. Thompson.** 2005. ATP citrate lyase is an important component of cell growth and transformation. Oncogene **24:**6314–6322.
10. **Beigneux, A. P., C. Kosinski, B. Gavino, J. D. Horton, W. C. Skarnes, and S. G. Young.** 2004. ATP-citrate lyase deficiency in the mouse. J. Biol. Chem. **279:**9557–9564.
11. **Benjamini, Y., and Y. Hochberg.** 1995. Controlling the false discovery rate: a practical and powerful approach to multiple testing. J. R. Stat. Soc. **57:**289–300.
12. **Cantwell, C. A., E. Sterneck, and P. F. Johnson.** 1998. Interleukin-6-specific activation of the C/EBPδ gene in hepatocytes is mediated by Stat3 and Sp1. Mol. Cell. Biol. **18:**2108–2117.
13. **Cen, B., A. Selvaraj, R. C. Burgess, J. K. Hitzler, Z. Ma, S. W. Morris, and R. Prywes.** 2003. Megakaryoblastic leukemia 1, a potent transcriptional co-activator for serum response factor (SRF), is required for serum induction of SRF target genes. Mol. Cell. Biol. **23:**6597–6608.
14. **Chapman, R. S., E. K. Duff, P. C. Lourenco, E. Tonner, D. J. Flint, A. R. Clarke, and C. J. Watson.** 2000. A novel role for IRF-1 as a suppressor of apoptosis. Oncogene **19:**6386–6391.
15. **Chapman, R. S., P. Lourenco, E. Tonner, D. Flint, S. Selbert, K. Takeda, S. Akira, A. R. Clarke, and C. J. Watson.** 2000. The role of Stat3 in apoptosis and mammary gland involution. Conditional deletion of Stat3. Adv. Exp. Med. Biol. **480:**129–138.
16. **Chapman, R. S., P. C. Lourenco, E. Tonner, D. J. Flint, S. Selbert, K. Takeda, S. Akira, A. R. Clarke, and C. J. Watson.** 1999. Suppression of epithelial apoptosis and delayed mammary gland involution in mice with a conditional knockout of Stat3. Genes Dev. **13:**2604–2616.
17. **Chen, J., C. M. Kitchen, J. W. Streb, and J. M. Miano.** 2002. Myocardin: a component of a molecular switch for smooth muscle differentiation. J. Mol. Cell. Cardiol. **34:**1345–1356.
18. **Clarkson, R. W., M. T. Wayland, J. Lee, T. Freeman, and C. J. Watson.** 2004. Gene expression profiling of mammary gland development reveals putative roles for death receptors and immune mediators in post-lactational regression. Breast Cancer Res. **6:**R92–R109.
19. **Copeland, J., and R. Treisman.** 2002. Activation of SRF by the diaphanous related formin mDia1 is mediated by its effects on actin polymerization. Mol. Biol. Cell **13:**4088–4099.
20. **Du, K. L., M. Chen, J. Li, J. J. Lepore, P. Mericko, and M. S. Parmacek.** 2004. Megakaryoblastic leukemia factor-1 transduces cytoskeletal signals and induces smooth muscle cell differentiation from undifferentiated embryonic stem cells. J. Biol. Chem. **279:**17578–17586.
21. **Du, K. L., H. S. Ip, J. Li, M. Chen, F. Dandre, W. Yu, M. M. Lu, G. K. Owens, and M. S. Parmacek.** 2003. Myocardin is a critical serum response factor cofactor in the transcriptional program regulating smooth muscle cell differentiation. Mol. Cell. Biol. **23:**2425–2437.
22. **Dundas, S. R., M. G. Ormerod, B. A. Gusterson, and M. J. O'Hare.** 1991. Characterization of luminal and basal cells flow-sorted from the adult rat mammary parenchyma. J. Cell Sci. **100:**459–471.
23. **Frith, M. C., Y. Fu, L. Yu, J. F. Chen, U. Hansen, and Z. Weng.** 2004. Detection of functional DNA motifs via statistical over-representation. Nucleic Acids Res. **32:**1372–1381.
24. **Fujita, N., K. Susuki, M. T. Vanier, B. Popko, N. Maeda, A. Klein, M. Henseler, K. Sandhoff, H. Nakayasu, and K. Suzuki.** 1996. Targeted disruption of the mouse sphingolipid activator protein gene: a complex multiple phenotype, including severe leukodystrophy and wide-spread storage of multiple sphingolipids. Hum. Mol. Genet. **5:**711–725.
25. **Furth, P. A., U. Bar-Peled, and M. Li.** 1997. Apoptosis and mammary gland involution: reviewing the process. Apoptosis **2:**19–24.
26. **Gasmi, L., and A. G. McLennan.** 2001. The mouse Nudt7 gene encodes a peroxisomal nudix hydrolase specific for coenzyme A and its derivatives. Biochem. J. **357:**33–38.
27. **Gentleman, R. C., V. J. Carey, D. M. Bates, B. Bolstad, M. Dettling, S. Dudoit, B. Ellis, L. Gautier, Y. Ge, J. Gentry, K. Hornik, T. Hothorn, W. Huber, S. Iacus, R. Irizarry, F. Leisch, C. Li, M. Maechler, A. J. Rossini, G. Sawitzki, C. Smith, G. Smyth, L. Tierney, J. Y. Yang, and J. Zhang.** 2004. Bioconductor: open software development for computational biology and bioinformatics. Genome Biol. **5:**R80.
28. **Gineitis, D., and R. Treisman.** 2001. Differential usage of signal transduction pathways defines two types of serum response factor target gene. J. Biol. Chem. **276:**24531–24539.
29. **Gusterson, B. A., P. Monaghan, R. Mahendran, J. Ellis, and M. J. O'Hare.** 1986. Identification of myoepithelial cells in human and rat breasts by anti-common acute lymphoblastic leukemia antigen antibody A12. JNCI **77:**343–349.
30. **Hill, C. S., J. Wynne, and R. Treisman.** 1995. The Rho family GTPases RhoA, Rac1, and CDC42Hs regulate transcriptional activation by SRF. Cell **81:**1159–1170.
31. **Humphreys, R. C., B. Bierie, L. Zhao, R. Raz, D. E. Levy, and L. Hennighausen.** 2002. Deletion of Stat3 blocks mammary gland involution and extends functional competence of the secretory epithelium in the absence of lactogenic stimuli. Endocrinology **143:**3641–3650.
32. **Hutt, J. A., J. P. O'Rourke, and J. DeWille.** 2000. Signal transducer and activator of transcription 3 activates CCAAT enhancer-binding protein delta gene transcription in G0 growth-arrested mouse mammary epithelial cells and in involuting mouse mammary gland. J. Biol. Chem. **275:**29123–29131.
33. **Jain, N., J. Thatte, T. Braciale, K. Ley, M. O'Connell, and J. K. Lee.** 2003. Local pooled-error test for identifying differentially expressed genes with a small number of replicated microarrays. Bioinformatics **19:**1945–1951.
34. **Johansen, F. E., and R. Prywes.** 1995. Serum response factor: transcriptional regulation of genes induced by growth factors and differentiation. Biochim. Biophys. Acta **1242:**1–10.
35. **Leist, M., and M. Jaatela.** 2001. Four deaths and a funeral: from caspases to alternative mechanisms. Nat. Rev. Mol. Cell Biol. **2:**1–10.
36. **Leung, K., A. Nagy, I. Gonzalez-Gomez, J. Groffen, N. Heisterkamp, and V. Kaartinen.** 2003. Targeted expression of activated Rac3 in mammary epithelium leads to defective postlactational involution and benign mammary gland lesions. Cells Tissues Organs **175:**72–83.
37. **Li, J., X. Zu, M. Chen, L. Cheng, D. Zhou, M. M. Lu, K. Du, J. A. Epstein, and M. S. Parmacek.** 2005. Myocardin-related transcription factor B is required in cardiac neural crest for smooth muscle differentiation and cardiovascular development. Proc. Natl. Acad. Sci. USA **102:**8916–8921.

37a. **Li, S., S. Chang, X. Qi, J. A. Richardson, and E. N. Olson.** 2006. Requirement of a myocardin-related transcription factor for development of mammary epithelial cells. Mol. Cell. Biol. **26:**5797–5808.

38. **Li, S., D. Z. Wang, Z. Wang, J. A. Richardson, and E. N. Olson.** 2003. The serum response factor coactivator myocardin is required for vascular smooth muscle development. Proc. Natl. Acad. Sci. USA **100:**9366–9370.
39. **Li, S., M. P. Czubryt, J. McAnally, R. Bassel-Duby, J. A. Richardson, F. F. Wiebel, A. Nordheim, and E. N. Olson.** 2005. Requirement for serum response factor for skeletal muscle growth and maturation revealed by tissue-specific gene deletion in mice. Proc. Natl. Acad. Sci. USA **102:**1082–1087.
40. **Linzell, J. L.** 1955. Some observations on the contractile tissue of the mammary glands. J. Physiol. **130:**257–267.
41. **Ma, Z., S. W. Morris, V. Valentine, M. Li, J. A. Herbrick, X. Cui, D. Bouman, Y. Li, P. K. Mehta, D. Nizetic, Y. Kaneko, G. C. Chan, L. C. Chan, J. Squire, S. W. Scherer, and J. K. Hitzler.** 2001. Fusion of two novel genes, RBM15

and MKL1, in the t(1;22)(p13;q13) of acute megakaryoblastic leukemia. Nat. Genet. **28:**220–221.
42. **Mahendran, R. S., M. J. O'Hare, M. G. Ormerod, P. A. Edwards, R. A. McIlhinney, and B. A. Gusterson.** 1989. A new monoclonal antibody to a cell-surface antigen that distinguishes luminal epithelial and myoepithelial cells in the rat mammary gland. J. Cell Sci. **94:**545–552.
43. **Manabe, I., M. Kurabayashi, Y. Shimomura, M. Kuro-o, N. Watanabe, M. Watanabe, M. Aikawa, T. Suzuki, Y. Yazaki, and R. Nagai.** 1997. Isolation of the embryonic form of smooth muscle myosin heavy chain (SMemb/NMHC-B) gene and characterization of its 5′-flanking region. Biochem. Biophys. Res. Commun. **239:**598–605.
44. **Manabe, I., and G. K. Owens.** 2001. CArG elements control smooth muscle subtype-specific expression of smooth muscle myosin in vivo. J. Clin. Investig. **107:**823–834.
45. **Marti, A., Z. Feng, H. J. Altermatt, and R. Jaggi.** 1997. Milk accumulation triggers apoptosis of mammary epithelial cells. Eur. J. Cell Biol. **73:**158–165.
46. **Matys, V., E. Fricke, R. Geffers, E. Gossling, M. Haubrock, R. Hehl, K. Hornischer, D. Karas, A. E. Kel, O. V. Kel-Margoulis, D. U. Kloos, S. Land, B. Lewicki-Potapov, H. Michael, R. Munch, I. Reuter, S. Rotert, H. Saxel, M. Scheer, S. Thiele, and E. Wingender.** 2003. TRANSFAC: transcriptional regulation, from patterns to profiles. Nucleic Acids Res. **31:**374–378.
47. **Mercher, T., M. Busson-Le Coniat, F. N. Khac, P. Ballerini, M. Mauchauffe, H. Bui, B. Pellegrino, I. Radford, F. Valensi, F. Mugneret, N. Dastugue, O. A. Bernard, and R. Berger.** 2002. Recurrence of OTT-MAL fusion in t(1;22) of infant AML-M7. Genes Chromosomes Cancer **33:**22–28.
48. **Mercher, T., M. B. Coniat, R. Monni, M. Mauchauffe, F. N. Khac, L. Gressin, F. Mugneret, T. LeBlanc, N. Dastugue, R. Berger, and O. A. Bernard.** 2001. Involvement of a human gene related to the Drosophila spen gene in the recurrent t(1;22) translocation of acute megakaryocytic leukemia. Proc. Natl. Acad. Sci. USA **98:**5776–5779.
49. **Miano, J. M.** 2003. Serum response factor: toggling between disparate programs of gene expression. J. Mol. Cell. Cardiol. **35:**577–593.
50. **Miralles, F., G. Posern, A. I. Zaromytidou, and R. Treisman.** 2003. Actin dynamics control SRF activity by regulation of its coactivator MAL. Cell **113:**329–342.
51. **Nagato, T., H. Yoshida, A. Yoshida, and Y. Uehara.** 1980. A scanning electron microscope study of myoepithelial cells in exocrine glands. Cell Tissue Res. **209:**1–10.
52. **Nakagawa, T., S. Shimizu, T. Watanabe, O. Yamaguchi, K. Otsu, H. Yamagata, H. Inohara, T. Kubo, and Y. Tsujimoto.** 2005. Cyclophilin D-dependent mitochondrial permeability transition regulates some necrotic but not apoptotic cell death. Nature **434:**652–658.
53. **Nakamura, M., W. Nishida, S. Mori, K. Hiwada, K. Hayashi, and K. Sobue.** 2001. Transcriptional activation of beta-tropomyosin mediated by serum response factor and a novel Barx homologue, Barx1b, in smooth muscle cells. J. Biol. Chem. **276:**18313–18320.
54. **Nakano, H., K. Furuya, and S. Yamagishi.** 2001. Synergistic effects of ATP on oxytocin-induced intracellular Ca^{2+} response in mouse mammary myoepithelial cells. Pfluegers Arch. Eur. J. Physiol. **442:**57–63.
55. **Norman, C., M. Runswick, R. Pollock, and R. Treisman.** 1988. Isolation and properties of cDNA clones encoding SRF, a transcription factor that binds to the c-fos serum response element. Cell **55:**989–1003.
56. **Oh, J., J. A. Richardson, and E. N. Olson.** 2005. Requirement of myocardin-related transcription factor-B for remodeling of branchial arch arteries and smooth muscle differentiation. Proc. Natl. Acad. Sci. USA **102:**15122–15127.
57. **O'Hare, M. J., M. G. Ormerod, P. Monaghan, E. B. Lane, and B. A. Gusterson.** 1991. Characterization in vitro of luminal and myoepithelial cells isolated from the human mammary gland by cell sorting. Differentiation **46:**209–221.
58. **Palmieri, F., F. Bisaccia, L. Capobianco, V. Dolce, G. Fiermonte, V. Iacobazzi, C. Indiveri, and L. Palmieri.** 1996. Mitochondrial metabolite transporters. Biochim. Biophys. Acta **1275:**127–132.
59. **Parmacek, M. S.** 2001. Transcriptional programs regulating vascular smooth muscle cell development and differentiation. Curr. Top. Dev. Biol. **51:**69–89.
60. **Pitelka, D. R., S. T. Hamamoto, J. G. Duafala, and M. K. Nemanic.** 1973. Cell contacts in the mouse mammary gland. I. Normal gland in postnatal development and the secretory cycle. J. Cell Biol. **56:**797–818.
61. **Ray, A., M. Hannink, and B. K. Ray.** 1995. Concerted participation of NF-κB and C/EBP heteromer in lipopolysaccharide induction of serum amyloid A gene expression in liver. J. Biol. Chem. **270:**7365–7374.
62. **Rudland, P. S., and C. M. Hughes.** 1989. Immunocytochemical identification of cell types in human mammary gland: variations in cellular markers are dependent on glandular topography and differentiation. J. Histochem. Cytochem. **37:**1087–1100.
63. **Sasazuki, T., T. Sawada, S. Sakon, T. Kitamura, T. Kishi, T. Okazaki, M. Katano, M. Tanaka, M. Watanabe, H. Yagita, K. Okumura, and H. Nakano.** 2002. Identification of a novel transcriptional activator, BSAC, by a functional cloning to inhibit tumor necrosis factor-induced cell death. J. Biol. Chem. **277:**28853–28860.
64. **Selvaraj, A., and R. Prywes.** 2003. Megakaryoblastic leukemia-1/2, a transcriptional co-activator of serum response factor, is required for skeletal myogenic differentiation. J. Biol. Chem. **278:**41977–41987.
65. **Selvaraj, A., and R. Prywes.** 2004. Expression profiling of serum inducible genes identifies a subset of SRF target genes that are MKL dependent. BMC Mol. Biol. **5:**13.
66. **Shillingford, J. M., K. Miyoshi, G. W. Robinson, B. Bierie, Y. Cao, M. Karin, and L. Hennighausen.** 2003. Proteotyping of mammary tissue from transgenic and gene knockout mice with immunohistochemical markers: a tool to define developmental lesions. J. Histochem. Cytochem. **51:**555–565.
67. **Shore, P., and A. D. Sharrocks.** 1995. The MADS-box family of transcription factors. Eur. J. Biochem. **229:**1–13.
68. **Smith, C. E., and D. A. Johnson.** 1985. Human bronchial leucocyte proteinase inhibitor. Rapid isolation and kinetic analysis with human leucocyte proteinases. Biochem. J. **225:**463–472.
69. **Somogyi, K., and P. Rorth.** 2004. Evidence for tension-based regulation of Drosophila MAL and SRF during invasive cell migration. Dev. Cell **7:**85–93.
70. **Sotiropoulos, A., D. Gineitis, J. Copeland, and R. Treisman.** 1999. Signal-regulated activation of serum response factor is mediated by changes in actin dynamics. Cell **98:**159–169.
71. **Stein, T., J. S. Morris, C. R. Davies, S. J. Weber-Hall, M. A. Duffy, V. J. Heath, A. K. Bell, R. K. Ferrier, G. P. Sandilands, and B. A. Gusterson.** 2004. Involution of the mouse mammary gland is associated with an immune cascade and an acute-phase response, involving LBP, CD14 and STAT3. Breast Cancer Res. **6:**R75–R91.
72. **Storey, J. D., and R. Tibshirani.** 2003. Statistical significance for genome-wide studies. Proc. Natl. Acad. Sci. USA **100:**9440–9445.
73. **Taleisnik, S., and R. Orias.** 1966. Pituitary melanocyte-stimulating hormone (MSH) after suckling stimulus. Endocrinology **78:**522–526.
74. **Tonner, E., M. C. Barber, G. J. Allan, J. Beattie, J. Webster, C. B. Whitelaw, and D. J. Flint.** 2002. Insulin-like growth factor binding protein-5 (IGFBP-5) induces premature cell death in the mammary glands of transgenic mice. Development **129:**4547–4557.
75. **Treisman, R.** 1994. Ternary complex factors: growth factor regulated transcriptional activators. Curr. Opin. Genet. Dev. **4:**96–101.
76. **Wang, D., P. S. Chang, Z. Wang, L. Sutherland, J. A. Richardson, E. Small, P. A. Krieg, and E. N. Olson.** 2001. Activation of cardiac gene expression by myocardin, a transcriptional cofactor for serum response factor. Cell **105:**851–862.
77. **Wang, D., R. Passier, Z. P. Liu, C. H. Shin, Z. Wang, S. Li, L. B. Sutherland, E. Small, P. A. Krieg, and E. N. Olson.** 2002. Regulation of cardiac growth and development by SRF and cofactors. Cold Spring Harbor Symp. Quant. Biol. **67:**97–105.
78. **Wang, D. Z., S. Li, D. Hockemeyer, L. Sutherland, Z. Wang, G. Schratt, J. A. Richardson, A. Nordheim, and E. N. Olson.** 2002. Potentiation of serum response factor activity by a family of myocardin-related transcription factors. Proc. Natl. Acad. Sci. USA **99:**14855–14860.
79. **Wang, D. Z., and E. N. Olson.** 2004. Control of smooth muscle development by the myocardin family of transcriptional coactivators. Curr. Opin. Genet. Dev. **14:**558–566.
80. **Wang, Z., D.-Z. Wang, G. C. Teg Pipes, and E. N. Olson.** 2003. Myocardin is a master regulator of smooth muscle gene expression. Proc. Natl. Acad. Sci. USA **100:**7129–7134.
81. **Weiss, J. M., P. Korge, H. M. Honda, and P. Ping.** 2003. Role of the mitochondrial permeability transition in myocardial disease. Circ. Res. **93:**292–301.
82. **Yoshida, T., S. Sinha, F. Dandre, B. R. Wamhoff, M. H. Hoofnagle, B. E. Kremer, D. Z. Wang, E. N. Olson, and G. K. Owens.** 2003. Myocardin is a key regulator of CArG-dependent transcription of multiple smooth muscle marker genes. Circ. Res. **92:**856–864.
83. **Zhang, S. X., E. Garcia-Gras, D. R. Wycuff, S. J. Marriot, N. Kadeer, W. Yu, E. N. Olson, D. J. Garry, M. S. Parmacek, and R. J. Schwartz.** 2005. Identification of direct serum-response factor gene targets during Me2SO-induced P19 cardiac cell differentiation. J. Biol. Chem. **280:**19115–19126.